JOURNAL OF THE MECHANICAL BEHAVIOR OF BIOMEDICAL MATERIALS 41 (2015) 336–356

Available online at www.sciencedirect.com

ScienceDirect

www.elsevier.com/locate/jmbbm

Research Paper

The evaluation of new multi-material human soft tissue simulants for sports impact surrogates

Thomas Payne[a], *Séan Mitchell*[a,*], *Richard Bibb*[b], *Mark Waters*[c]

[a]*Sports Technology Institute, Loughborough University, UK*
[b]*Loughborough Design School, Loughborough University, UK*
[c]*School of Dentistry, Cardiff University, UK*

ARTICLE INFO

Article history:
Received 30 April 2014
Received in revised form
3 September 2014
Accepted 19 September 2014
Available online 30 September 2014

Keywords:
Polydimethysiloxane
Surrogate
Sports
Impact
Simulant
FEA
Thigh
Silicone

ABSTRACT

Previous sports impact reconstructions have highlighted the inadequacies in current measures to evaluate the effectiveness of personal protective equipment (PPE) and emphasised the need for improved impact surrogates that provide a more biofidelic representation of human impact response.

The skin, muscle and subcutaneous adipose tissues were considered to constitute the structures primarily governing the mechanical behaviour of the human body segment. A preceding study by Payne et al. (in press) investigated the formulation and characterisation of muscle tissue simulants. The present study investigates the development of bespoke blends of additive cure polydimethysiloxane (PDMS) silicones to represent both skin and adipose tissues using the same processes previously reported. These simulants were characterised mechanically through a range of strain rates and a range of hyperelastic and viscoelastic constitutive models were evaluated to describe their behaviour.

To explore the worth of the silicone simulants, finite element (FE) models were developed using anthropometric parameters representative of the human thigh segment, derived from the Visible Human Project. The multi-material silicone construction was validated experimentally and compared with both organic tissue data from literature and commonly used single material simulants: Dow Corning Silastic 3480 series silicones and ballistics gelatin when subject to a representative sports specific knee impact. Superior biofidelic performance is reported for the PDMS silicone formulations and surrogate predictions.

1. Introduction

1.1. Background

In sports, impact injuries are a common occurrence. Human surrogates are required to provide both an assessment of injury risk and evaluation of the effectiveness of personal protective equipment (PPE). Artificial impact surrogates are widely used for this purpose and can be broadly divided into two categories: computational and synthetic surrogates.

Within the sporting goods industry, synthetic surrogates are required to provide a physical interface to affix PPE and

*Corresponding author. Tel.: +44 1509 564804; fax: +44 1509 564801
E-mail address: s.r.mitchell@lboro.ac.uk (S. Mitchell).

http://dx.doi.org/10.1016/j.jmbbm.2014.09.018
1751-6161/

evaluate real damage mechanisms. The surrogates must also be capable of providing feedback of the mechanical phenomena occurring through instrumentation; this is commonly in the form of pressure films, strain gauges, load cells and accelerometers. However, synthetic surrogates can be expensive and experimental trials can be time consuming. The instrumentation generally offers a partial performance assessment and can introduce artificial stress concentrations affecting the biofidelity of the surrogate.

Computational finite element (FE) models present a method of studying complex mechanical interactions without introducing artificial foreign bodies and can provide a more continuous description of tissue behaviour (e.g. stress profiles). Superior research in this field is, therefore, likely to be based on complimentary mutually validating synthetic and computational human surrogate models providing a greater confidence in each of the approaches (Payne et al., 2013).

Current synthetic impact surrogates are typically categorised as either "durable" or "frangible". Non-frangible surrogates often differ by industry application and either use stiff, durable materials, relying on instrumentation to assess rigid segment response with respect to organ damage (e.g. automotive crash test dummies) or use a combination of a stiff skeletal component and a single durable simulant to represent the composite response of all soft tissues. Mechanical sports impact surrogates have previously used Silastic 3480 series (Dow Corning Corporation, Michigan, USA) silicones (Hrysomallis, 2009) as single soft tissue simulants and they have since been used elsewhere in industry. Alternatively, frangible surrogates typically offer greater biofidelity but are intended for single use and predominantly exploit visible damage modes to indicate potential human injuries. In the military, ballistics gelatin has served as a universal soft tissue simulant for several decades (Fackler, 1988; Sellier and Kneubuehl, 1994) and is either mixed in 10% (FBI protocol, Fackler, 1988) or 20% (NATO protocol) gelatin concentrations (by mass).

It is suggested that these single soft tissue material constructions overlook important mechanical phenomena experienced between soft tissue layers such as variable stiffness, relative movement between structures, pressure distribution and deformation of tissues distant from the impact site. For the sporting goods industry it is believed that a durable mechanical surrogate presents the best method for practically evaluating PPE. A list of desirable characteristics for an effective sports impact surrogate was outlined by Payne et al. (2013):

- Tissue structure biofidelity: the surrogate needs to represent the key human structural elements so specific injury outcomes can be explored.
- Tissue impact response biofidelity: the structures should have comparable strength and stiffness properties to approximate human behaviour on impact.
- Instrumentation capabilities: to provide accurate feedback mechanisms to correlate the impact parameters to specific injury outcomes.
- Durability: capable of providing consistent results from repeated impacts.

Skin, muscle and subcutaneous adipose tissues are considered the primary soft tissue structures governing the mechanical impact response of the human body in fleshy regions prone to bruising. It is proposed that a multi-material surrogate embodying a combination of these tissues can elicit a more biofidelic impact response.

A preceding study by Payne et al. (in press) showed the potential of using polydimethysiloxane (PDMS) silicones to match specific mechanical properties of human muscle. The current study presents an investigation into the benefits of a multi-material surrogate when compared to previously used single material simulants. Adipose and skin simulants have been fabricated and mechanically tested using the procedures outlined in Payne et al. (in press). The mechanical behaviour of both simulants have been characterised using a range of hyperelastic material models and a viscoelastic Prony series. The worth and external validity of the multi-material surrogate has been demonstrated using FE models comparing single material constructions to multi-material models. Simple, cost effective, single and multi-material puck specimens have been constructed physically and the accuracy of corresponding puck FE model predictions have been established for sport relevant impact performance. The potential benefits of a simplified multi-layer thigh segment surrogate have been explored using a more complex FE model subjected to a knee-on-thigh impact, with reference to idealised human tissue behaviour predictions and alternate surrogate material alternatives, to establish the merit of further research to develop a superior physical multi-layer human thigh surrogate.

1.2. *Structure and composition of organic tissues*

1.2.1. *Skin*

Skin is the outermost layer of tissue on the human body and represents a protective barrier from mechanical trauma and a stiff interface surrounding other tissues (Edwards and Marks, 1995; Pailler-Mattei et al., 2008). With the exception of muscle and skeletal tissues it represents the largest organ, constituting approximately 5.5% of body mass (Goldsmith, 1990). It consists of two major structures, the dermis and epidermis, though the structural response is largely determined by the dermal layer, which is primarily populated by collagen fibres (75% of dry weight). The fibres at rest are twisted and knotted in a very complex network with interspersed elastin fibres and lymphatic elements (Pailler-Mattei et al., 2008; Wu et al., 2003); this makes the fibres very stiff in tension but able to carry little load in compression. Skin properties are greatly inhomogeneous, non-elastic, time-dependent and in a state of biaxial tension in vivo. Its properties are based on the concentration and the orientation of the collagen fibres (Edwards and Marks, 1995; Wu et al., 2003; Flynn and Mccormack, 2008; Lim et al., 2011; Ní Annaidh et al., 2012).

Most skin characterisation studies have been conducted on porcine tissue which has been shown to exhibit comparable histological, physiological and structural properties to humans (Schmook et al., 2001; Avon and Wood, 2005; Shergold et al., 2006). The mechanical behaviour observed is influenced by many factors relating to both the specimen and loading conditions. Skin exhibits significant anisotropy

underpinned by the presence of Langer lines which describe natural lines of pre-tension in the skin and have a significant effect on the mechanical response (Edwards and Marks, 1995; Ní Annaidh et al., 2012). Liu and Yeung (2008) observed a greater stress relaxation in specimens cut perpendicular to the fibre direction and a greater viscoelasticity at higher strains. Similarly Ankersen et al. (1999) and Lim et al. (2011) observed a clear distinction in material stiffness in tensile tests between the two orthogonal directions. The age of the mammalian surrogate is also a pertinent consideration; the collagen content of skin decreases with age and young skin is typically less protective against large strain trauma than older skin which has a proportionally greater elastic region. Older skin also has a lower water content, which has a significant effect on its viscous response (Potts et al., 1984). The location from which the specimens are taken has also been shown to have a significant effect on properties (Haut, 1989; Sugihara et al., 1991; Ní Annaidh et al. 2012).

The loading conditions such as mechanical loading type, loading rate and temperature can influence response. The morphology of the tissue results in loading type dependent behaviour whereby skin exhibits a greater stiffness in compression than in tension (Lanir and Fung, 1974; Dunn et al., 1985), though this response can differ between in vivo and in vitro studies. The mechanical properties of skin are also highly dependent on loading rate (Finlay, 1978; Potts et al., 1984; Jamison et al., 1968). At high loading rates a more viscous response has been observed (Jee and Komvopoulos, 2014), perhaps due to an increased fluid (blood, water, lymph) loss from the compressed dermis (Edwards and Marks, 1995).

The typical stress–strain response of skin can be divided into three regions, described by Brown (1973). In the initial region, the skin is compliant and large deformation occurs at low applied loads with the fibres largely unaligned, the constitutive response at this phase is largely governed by the bending stiffness of collagen fibres and viscous shear between the fibres and extrafibrillar matrix (Cohen et al., 1976). The second phase, the stiffness gradually increases as fibres align themselves in the direction of the load and in the third phase, skin behaves almost linearly with the stiffness increasing rapidly as the collagen fibres are mostly aligned and the response becomes dependent on the tensile mechanical response of the collagen fibres which are three orders of magnitude stiffer than the elastin fibres (Ní Annaidh et al., 2012); this region has been suggested as occurring at approximately 0.4 strain (Comley and Fleck, 2012).

Due to its thickness skin is commonly tested in tension (Wu et al., 2003) and under quasi-static loading conditions (e.g. Ankersen et al., 1999; Ní Annaidh et al., 2012), though quasi-static responses may not be simply extrapolated to high strain rates without experimental validation. Lim et al. (2011) and Gallagher et al. (2012) conducted dynamic tensile testing on porcine and human skin tissues respectively using a modified Split Hopkinson Pressure Bar (SHPB). A significant strain rate dependency was observed in both sets of tests, though there was a significant difference in the magnitude of stiffness reported, which has varied widely between previous studies. Few studies have been reported on skin tissues in compression in vitro; Wu et al. (2003) conducted in vitro compressive tests on porcine tissues from the upper neck and back and Shergold et al. (2006) tested porcine rump skin in uniaxial compression. Data from a subset of representative studies are shown in Fig. 1.

1.2.2. *Subcutaneous adipose tissue*

Subcutaneous adipose tissue, also known as the hypodermis, is a connective fatty tissue located between the dermis and the aponeuroses and fascia of muscles, and is bonded strongly to the dermis. It plays an important role as a mechanical load absorbing and distributing member that absorbs shock and protects against local stresses (Robbins et al., 1989; Miller-Young et al., 2002; Geerligs et al., 2008; Sims et al., 2010; Comley and Fleck, 2012; Alkhouli et al., 2013). Adipose consists of 90–99% triglyceride, with the remaining tissue containing 5–30% water and 2–3% proteins (Albright and Stern, 1998). The tissue is a loose association of lipid filled cells called white adipocytes (80 μm diameter approximately) held in two extracellular networks of collagen fibres penetrated by fibroblasts, neural and vascular cells, and multipotent progenitor cells (Geerligs et al., 2008; Young and Christman, 2012; Sommer et al., 2013). The smaller network is a reinforcement basement membrane, comprised of collagen fibres, which acts as the walls of a closed cell foam

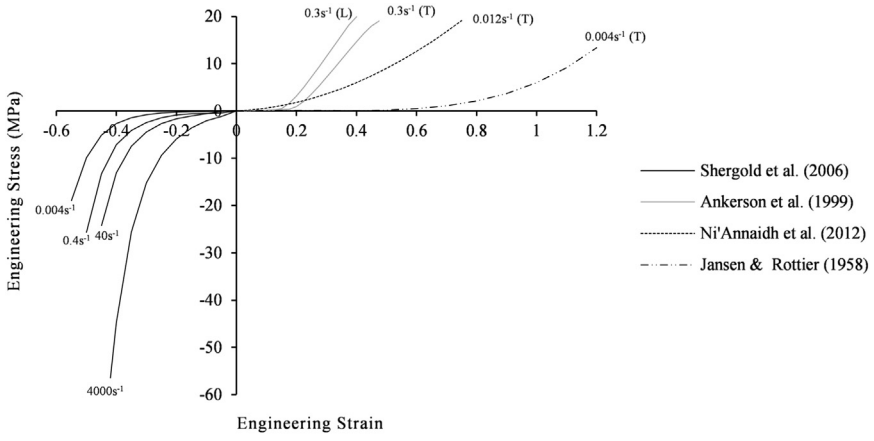

Fig. 1 – Engineering stress–strain graphs for a range of organic skin tissue samples at different strain rates (T – transverse; L – longitudinal).

with the adipocyte forming the cavity. The larger network is called the interlobular septa comprised of type I collagen fibres and is roughly 1 mm in size acting as an open celled foam (Comley and Fleck, 2010). Adipose, as with most biological tissues, exhibits heterogeneous, rate-dependent, viscoelastic behaviour and experiences large non-linear deformations (Holzapfel, 2004; Sapozhnikov and Ignatova, 2013). It is suggested that adipose is approximately isotropic in structure and due to the large liquid content is almost incompressible (Samani et al., 2003; Comley and Fleck, 2010), though a recent study by Sommer et al. (2013) observed some anisotropy in specimens.

In comparison to the relative wealth of research on the mechanical properties of skin, there is a paucity of studies characterising the response of adipose. Much of current research only presents linear material parameters (e.g. Young's modulus) at quasi-static strain rates whilst it is widely documented that the tissue exhibits a non-linear response and significant rate dependence (Comley and Fleck, 2012; Samani and Plewes, 2004; Alkhouli et al., 2013; Sommer et al., 2013).

Adipose is commonly characterised using samples from the human heel pad region (Miller-Young, et al., 2002; Erdemir et al., 2006; Natali et al., 2012), though fat pads on the hands and feet differ from subcutaneous tissues elsewhere in the body as they contain higher ratios of unsaturated versus saturated fatty acids (Geerligs et al., 2008). They also have morphological differences due to their anatomical function and high levels of stress experienced in normal loading conditions (Gefen and Haberman, 2007). In the heel pad, fat tissue is separated in a honeycomb structure of compartments (Fontanella et al., 2012).

Adipose properties have also been characterised using samples from human breast tissues (e.g. Azar et al., 2002; Krouskop et al., 1998; Van Houten et al., 2003; Sarvazyan et al., 1994; Samani et al., 2007) or porcine subcutaneous specimens (e.g. Geerligs et al., 2008; Comley and Fleck, 2010; Comley and Fleck, 2012), which have been shown to exhibit similarities in morphology, histology, and overall mechanical response with human tissues (Douglas, 1972; Paus et al., 2007).

Under compression adipose tissue has low stiffness initially (<0.3 strain) but then under higher loads the collagen fibres of fat and skin come under tension, restricting the movement of the adipose and increasing the stiffness (Miller-Young et al., 2002; Fontanella et al.,2012). This observation is supported by Alkhouli et al. (2013) who reported a mean elastic modulus of 1.6 ± 0.8 kPa up to 0.3 strain and a mean elastic modulus of 11.7 ± 6.4 kPa from 0.3 strain to failure. This theory was extended by Sapozhnikov and Ignatova (2013) who suggested that between 0.4 and 0.5 strain, adipose exhibits a non-linear behaviour followed by a transition section between 0.5 and 0.7 strain where stresses decrease attributed to the collapse of cell walls, with an expulsion of fluid. This is then followed by a hardening with a rapid unlimited increase in compressive stress governed by the stiffness of the remaining cell shells.

Under quasi-static strain rates, studies have shown the elastic modulus of adipose to be approximately between 1 and 4.5 kPa (Azar et al., 2002; Samani and Plewes, 2004; Samani et al., 2007; Sims et al., 2010; Comley and Fleck, 2012) with little strain rate sensitivities between 2×10^{-3} and $10\ s^{-1}$ (Comley and Fleck, 2012). Beyond $10\ s^{-1}$, significant sensitivity has been observed (Miller-Young et al., 2002; Gefen and Haberman, 2007; Comley and Fleck, 2012). Comley and Fleck (2012) reported an increase in Young's by three orders of magnitude from 2 kPa at $10\ s^{-1}$ to 4 MPa at $3000\ s^{-1}$, a similar modulus to the dermis. Comparable responses were observed by Egelbrektsson (2011) when conducting high strain rate compressive tests. Representative stress–strain data from a subset of characterisation studies are shown in Fig. 2.

1.3. *Aims and objectives*

Previously used surrogate materials do not accurately simulate human skin or adipose tissue structure or response. Their anisotropic, inhomogeneous, location, strain and strain rate dependent impact response behaviour is not accurately reproduced. Given inadequacies in current surrogates and measures of assessing PPE effectiveness (outlined in Payne et al., in press) there is a significant gulf between the current state-of-the-art durable surrogates and a fully biofidelic human surrogate.

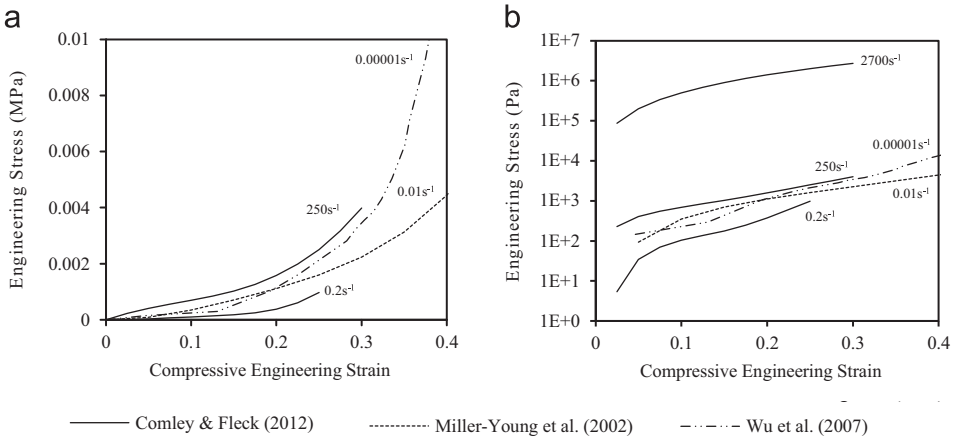

Fig. 2 – Compressive engineering stress–strain graphs for a range of organic adipose tissue samples at different strain rates in (a) linear and (b) log-linear plots.

A worthwhile intermediate step is to develop more biofidelic isotropic silicone materials which both provide improved accuracy of predictions and serve as a stepping stone to more biofidelic anisotropic materials. It can be argued that for specific applications a more limited level of biofidelity is adequate, in terms of injury related response phenomena simulation, and desirable, in terms of surrogate cost. The synthetic surrogate materials proposed in this study do not address the issue of anisotropy or local inhomogeneity. The materials are formulated in an attempt to exhibit superior biofidelity (especially in terms of strain and strain rate dependencies) for specific tissue types and to exhibit superior response distribution between tissue regions when assembled to form a multi-layer surrogate. The further worth of anisotropic material development can then be explored in a later study.

FE models can be effectively used as a diagnostic and predictive design tool to understand surrogate impact behaviours without having to construct expensive prototypes. In this study FE models have been used to provide an indication of predicted human impact behaviour through consideration of the compressive mechanical properties of key organic tissues from literature. This has enabled a comparison of the effectiveness of different materials.

The key research questions addressed by this study are as follows:

i. Can PDMS materials be fabricated that provide a better representation of organic skin and adipose tissues than other, commonly used, alternate simulant materials?
ii. Can experimental material characterisation, constitutive material modelling and dynamic FE load/deformation simulation techniques be used to accurately predict the performance of single and multi-material surrogate constructions using common and newly formulated synthetic surrogate materials?
iii. Does a multi-material PDMS silicone surrogate have the potential to mimic more closely multi-tissue organic human structures than current single surrogate material approaches?

2. Methodology

2.1. *Simulant formulation and characterisation*

2.1.1. *Formulations*

PDMS silicones were formulated using the techniques established in Payne et al. (in press). The silicone constituent parts were weighed and mixed manually prior to degassing in a vacuum chamber. The silicones were poured in an ASTM Standard D395 (2008) compressive specimen mould and cured in an environmental chamber at 90 °C. The Parts A and B PDMS silicone concentrations for skin and adipose simulants are shown in Table 1.

2.1.2. *Low strain rate mechanical tests*

The preceding study by Payne et al. (in press) describes the testing procedures used to characterise the simulants. Low strain rate uniaxial compressive tests were conducted using

Table 1 – Parts A and B silicone constituent concentrations (% by mass).

	Part A				Part B		Part A:B ratio
	Polymers			Catalyst (%)	H301 cross linker (%)	V31 polymer (%)	
	V46 (%)	V31 (%)	V21 (%)				
Skin	76.5	9.0	4.5	10	10	90	1:1
Adipose	46.8	21.6	21.6	10	10	90	10:1

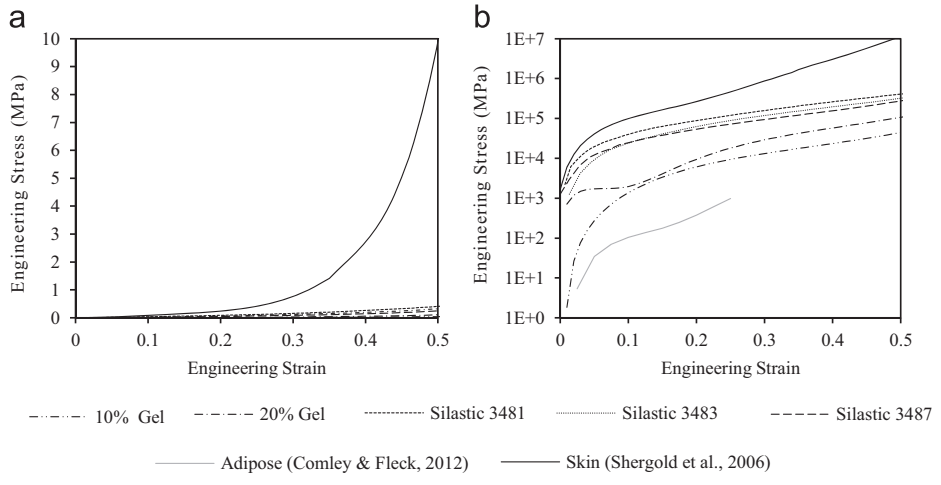

Fig. 3 – Quasi-static stress–strain graphs showing the uniaxial compressive responses of organic adipose (Comley and Fleck, 2012) and skin (Shergold et al., 2006) tissues compared to soft tissue simulants in (a) linear and (b) log-linear graphs.

an Instron 5569 screw-driven test machine. Tests were performed using a cyclic compressive protocol incrementally increasing the applied strain in 0.1 strain intervals to failure at a constant strain rate of 0.4 s^{-1}.

As an initial point of comparison, the quasi-static uniaxial compressive responses of organic skin and adipose tissues were compared to a range of commonly used soft tissue simulants (Fig. 3). Fig. 3 shows that skin is significantly stiffer than any simulant and adipose is significantly softer than any other simulant, particularly at strains greater than 0.1.

The quasi-static PDMS skin simulant response was compared to the best alternate simulant single material simulant (Silastic 3481) (Fig. 4). The PDMS skin simulant showed a consistently improved response compared to Silastic 3481 exhibiting differences between 84% and 90% of the organic tissue properties, whilst the Silastic simulant exhibited differences between 89% and 96%.

The quasi-static responses of the PDMS adipose simulant have been compared with organic tissue properties alongside the best alternate single material simulant (10% gelatin) (Fig. 5). The 10% gelatin simulant shows significant divergence from the target organic tissue dataset with an error of up to 1855% at 0.16 strain. The PDMS simulant exhibits a much closer response with a maximum of 239% error at 0.06 strain decreasing to 0% error at 0.23 strain.

The extent of the Mullins effect has been investigated with the percentage reductions in stress from cyclic compressive tests at maximal strain recorded. The skin simulant experienced a significantly lower stress softening effect than the adipose tissue simulant with percentage reductions of 3.9% and 13.5% respectively.

The poissons ratio of each simulant has been determined using high speed video of an ASTM D395 specimen in compression using the methods outlined in Payne et al. (in press). Both tissue simulants were determined to be quasi-incompressible with ratios of 0.476 and 0.492 for skin and adipose simulants respectively.

2.1.3. *Intermediate strain rate mechanical tests*

Intermediate strain rate compressive tests were conducted using an Instron 9250 drop tower using a 6.8 kg linear guided drop mass from a range of heights. The material response is recorded using three piezoelectric load cells in the base of the bottom compressive platen whilst the displacement of the

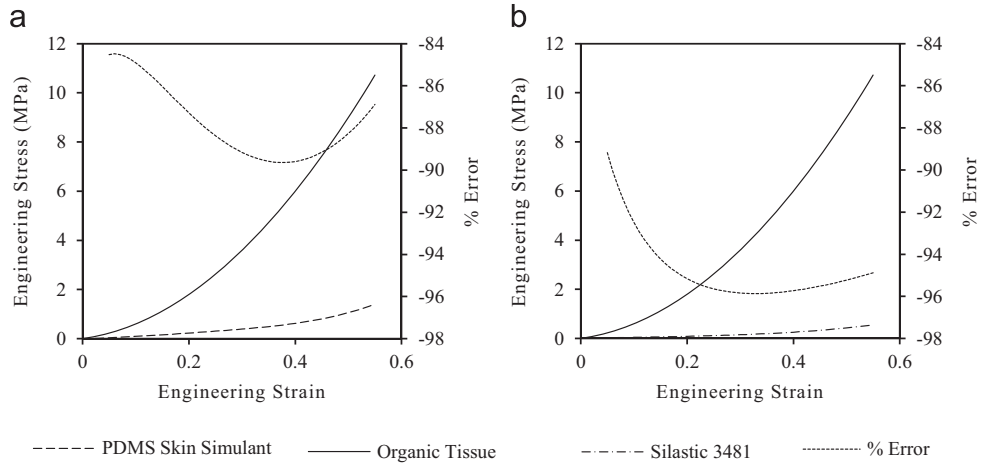

Fig. 4 – Quasi-static stress–strain graphs for: (a) PDMS skin simulant compared to organic skin tissue (Shergold et al., 2006) and (b) Silastic 3481 simulant compared to organic skin tissue (Shergold et al., 2006).

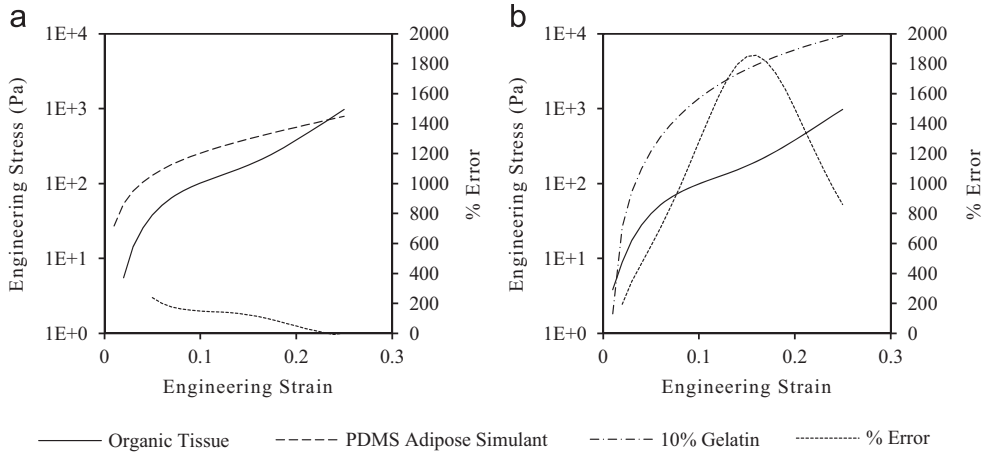

Fig. 5 – Log-linear quasi-static stress–strain graphs for (a) PDMS adipose simulant compared to organic adipose tissue (Comley and Fleck, 2012) and (b) 10% gelatin simulant compared to organic adipose tissue (Comley and Fleck, 2012).

specimen was recorded using high speed video. The stress–strain plots at a range of strain rates are shown in Fig. 6. The strain rates reported are characterised by the initial maximum value recorded; the differences in strain rate between materials varies due to differences in displacement rate.

At intermediate strain rates, the responses of the PDMS skin and adipose simulants were compared with the higher strain rate responses of the respective organic tissues by Shergold et al. (2006) and Comley and Fleck (2012); the banded lines indicate the PDMS responses (Fig. 7).

The responses of the PDMS skin tissue simulant falls within the response corridor outlined by the organic tissues. The adipose simulant, however, exhibited a greater stiffness than the organic equivalent, in particular at low strains and high strain rates. The organic tissues also appear to exhibit a greater strain hardening than the PDMS silicones at approximately 0.15 strain.

2.1.4. *Stress relaxation tests*

The viscoelasticity in the simulants was also determined using uniaxial stress-relaxation tests. Stress relaxation tests were performed on an Instron 5569 universal test machine using a ramp-and-hold compression test applying 0.5 strain to the specimen for 300 s. The relative differences in viscoelasticity are illustrated in normalised stress–time plots in Fig. 8 where it is clearly shown that the adipose simulant exhibited a far greater relaxation than the skin simulant.

2.2. *Constitutive modelling*

Hyperelastic and viscoelastic material models were used to describe the simulant materials. Mooney–Rivlin, Ogden and Neo Hookean hyperelastic models were fitted to the experimental data using the automated generator in Abaqus Explicit solver (Version 6.13). The material fits for both materials are shown in Fig. 9 alongside Table 2 showing the degree of

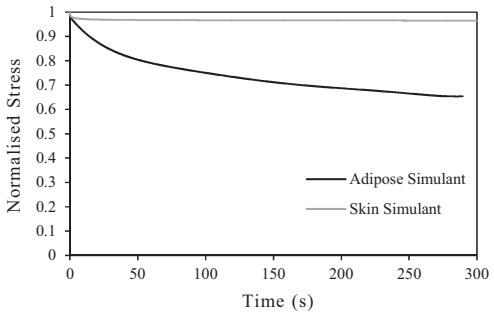

Fig. 8 – Normalised stress–time plot showing stress relaxation in PDMS skin and adipose tissue simulants.

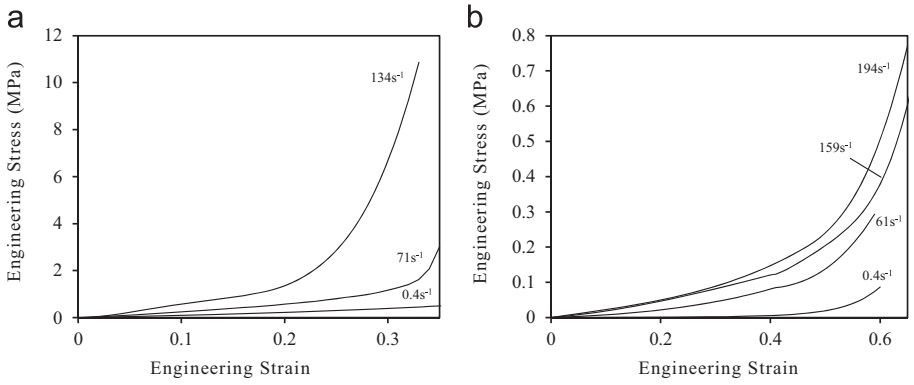

Fig. 6 – Intermediate strain rate engineering stress–strain curves for: (a) PDMS skin simulant and (b) PDMS adipose simulants.

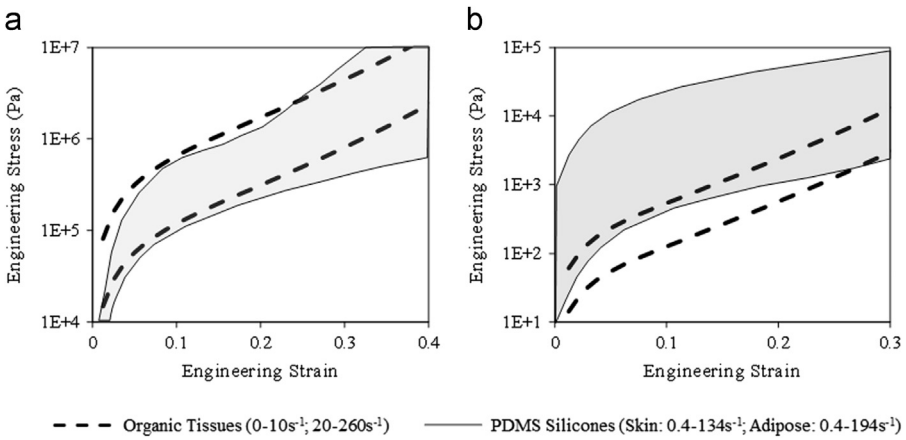

Fig. 7 – Log-linear engineering stress–strain graphs showing a comparison between PDMS simulants and organic tissue data at intermediate strain rates for (a) skin and (b) adipose tissues.

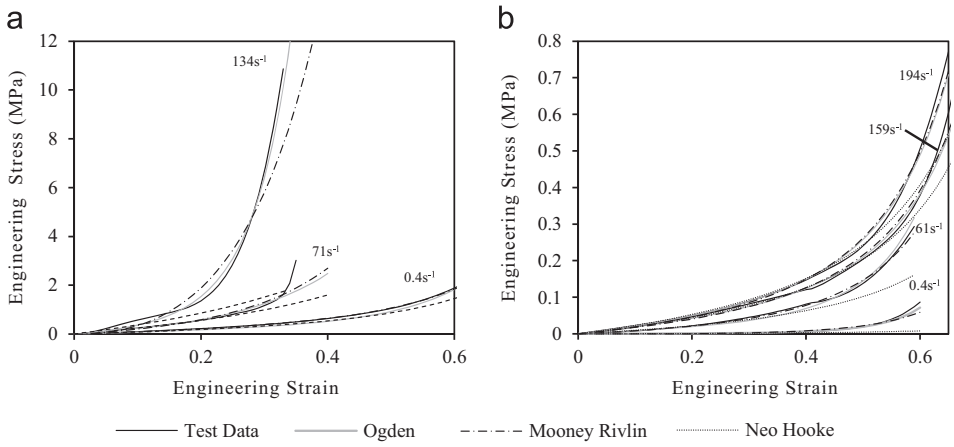

Fig. 9 – Hyperelastic model fits for (a) PDMS skin simulant and (b) PDMS adipose simulant at a range of intermediate strain rates.

Table 2 – Hyperelastic model coefficients for PDMS skin and adipose tissue simulants.

	Ogden		RMS error (MPa)	Mooney–Rivlin		RMS error (MPa)	Neo Hooke	RMS error (MPa)
	μ	α		C_{01}	C_{10}		C_{10}	
Skin								
0.4 s^{-1}	2.36×10^5	3.98	0.330	1.27×10^5	1.21×10^4	0.00771	1.24×10^5	0.035
71 s^{-1}	5.92×10^5	2.61	0.125	3.17×10^5	5.62×10^5	0.107	3.68×10^5	0.258
134 s^{-1}	7.40×10^5	9.41	0.311	5.24×10^6	5.18×10^6	1.41	5.62×10^5	3.94
Adipose								
0.4 s^{-1}	8.29×10^2	4.82	0.00209	4.42×10^3	3.79×10^3	0.00157	6.83×10^2	0.0145
61 s^{-1}	2.74×10^4	5.94	0.00773	2.55×10^3	9.19×10^3	0.00478	1.45×10^4	0.0364
159 s^{-1}	5.76×10^4	3.14	0.00806	2.00×10^4	5.35×10^3	0.0127	2.90×10^4	0.0184
194 s^{-1}	6.86×10^4	3.55	0.0131	1.76×10^4	9.90×10^3	0.0124	3.48×10^4	0.0521

divergence of each FE material prediction from the experimental data with root mean square (RMS) error values recorded to quantitatively show the closeness of fit.

The Ogden model generally provides the best description of the skin simulant which exhibits a significant strain hardening effect; this is most notable at 134 s^{-1} (0.311MPa RMS error). However, the softer adipose simulant, which experienced less strain hardening, is better represented by the Mooney–Rivlin model (<0.0127MPa RMS error).

A Prony series coefficients were also calculated for both simulants using data from the uniaxial stress relaxation tests (Table 3). Normalised shear modulus values were calculated from stress–strain data and used to generate time-dependent Prony series parameters in the automated feature of the FE solver which fits a curve to the stress relaxation data.

Table 3 – Prony series coefficients for PDMS skin and adipose tissue simuants.

i	g(i)	τ(i)
Skin		
1	2.67×10^{-2}	8.51×10^{-1}
2	8.07×10^{-3}	4.04×10^1
Adipose		
1	1.39×10^{-1}	7.51×10^{-5}
2	1.70×10^{-1}	3.07
3	7.41×10^{-2}	7.9×10^1

2.3. *Finite element models*

2.3.1. *Overview*

Finite element models were developed to illustrate the relative benefits of multi-material models compared to single material constructions. It is acknowledged that, the finite element models used only provide a very simplified representation of a limb segment, however their simplicity lends clarity to the observation of different impact responses when more or less representative organic tissue or synthetic surrogate material models are employed.

Two different surrogate geometries were designed: the first, a simple cylindrical puck to enable the cost effective experimental validation of the FE modelling methods; the second, a cylindrical thigh segment to predict the benefits of developing a multi-layer limb segment surrogate before incurring the expense of overcoming the manufacturing difficulties.

2.3.2. *Geometric parameters*

Surrogate dimensions (e.g. skin thickness) were determined from human anthropometric parameters derived from

measurement of axial CT scans of a 50th percentile US male from the visible human project (VHP, US National Library of Medicine). Distances from the bone centroid to tissue interfaces were sampled at 8 evenly distributed points on the cross section. This was performed at 5 sections through the length of the thigh region on the visible human project male scan and was used to infer average tissue distances from the bone centroid and hence thicknesses. A 130 mm diameter layered puck was designed to permit cost effective experimental validation under laboratory drop test conditions. A 150 mm diameter cylindrical surrogate was used to approximate the human thigh segment. The cylinder surrogate was given a length of 276 mm as it represents the largest fleshy area visible on the VHP scans where there were no other conflicting skeletal tissues (e.g. pelvis or patella bones). The surrogate geometries and dimensions are shown in Fig. 10, the bone ends in the cylinder surrogate were rigidly constrained in all translational directions.

2.3.3. *Material models*

Published organic tissue data for skin (Fig. 1), adipose (Fig. 2) and muscle tissue datasets presented in the preceding study (Payne et al., in press) were used as the initial basis for model definition. Relaxed muscle tissues were used instead of contracted as the impacts are believed to be more prevalent and serious when the participant would not be anticipating the impact. Data at representative intermediate strain rates for sports impact scenarios derived from cylindrical impact simulation of organic tissues were selected and used to populate material models (Fig. 11).

As previously discussed (Section 1.3), the complex organic tissue behaviour was approximated with isotropic and incompressible materials. Hence, single term Ogden models proposed by Shergold et al. (2006) and Comley and Fleck (2012) in 20–260 s^{-1} strain rate ranges were used to describe the compressive behaviour of the skin and adipose respectively. An Ogden model was created for muscle tissue using the dataset from previous studies by Mcelhaney (1966) and Song et al. (2007) (Table 4). The mechanical properties of bone were adapted from a quasi-static compressive experiment conducted by Mcelhaney (1966) on cortical bone. Cortical bone is significantly stiffer than trabecular bone (Rho et al., 1993) and it is believed that this constitutes a more significant part of the overall tissue response. An Ogden model fit for cortical bone is similarly detailed in Table 4; the densities of all the materials are also presented.

The viscoelastic properties of organic soft tissues are presented in the form of Quasi-Linear Viscoelastic (QLV) Prony Series (Table 5) using data adapted stress relaxation tests on skin (Wu et al., 2003); adipose (Gefen and Haberman, 2007) and relaxed muscle (Van Loocke et al., 2009).

The hyperelastic PDMS material models for each of the tissue structures at relevant strain rates are shown in Figure 11 alongside target organic tissue responses with material model coefficients detailled in Table 6.

Silastic 3480 series silicones have previously been used to represent human soft tissues. 3481, 3483 and 3487 two-part cure silicone elastomers were fabricated in the same manner as the PDMS silicones and characterised through a range of strain rates. Similarly, ballistics gelatin was formulated in 10% and 20% concentrations using the procedure outlined by Jussila (2004) and tested in the aforementioned manner. Data used to populate each of the hyperelastic material models are shown in Fig. 12 with hyperelastic model coefficients and viscoelastic Prony series coefficients detailed in Table 7.

2.3.4. *Sports impact scenarios*

A high-mass, low-velocity knee-on-thigh human impact similar to that which may be experienced in rugby or basketball gameplay was approximated using a 72 mm diameter, 3 kg hemispherical geometry with an initial velocity of 3 ms^{-1} adpated from Halkon et al. (2014).

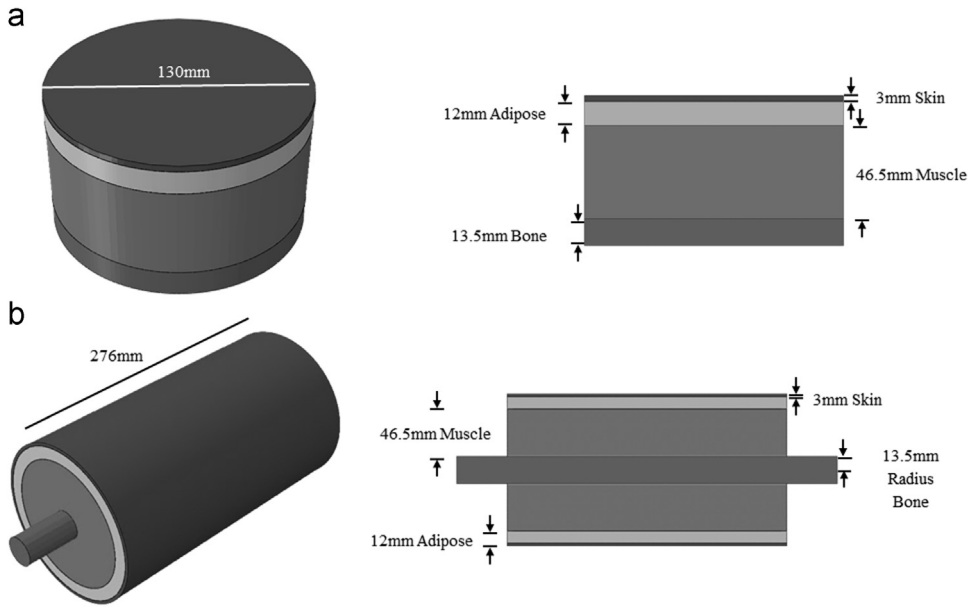

Fig. 10 – Surrogate geometric configurations for (a) layered puck and (b) cylinder models.

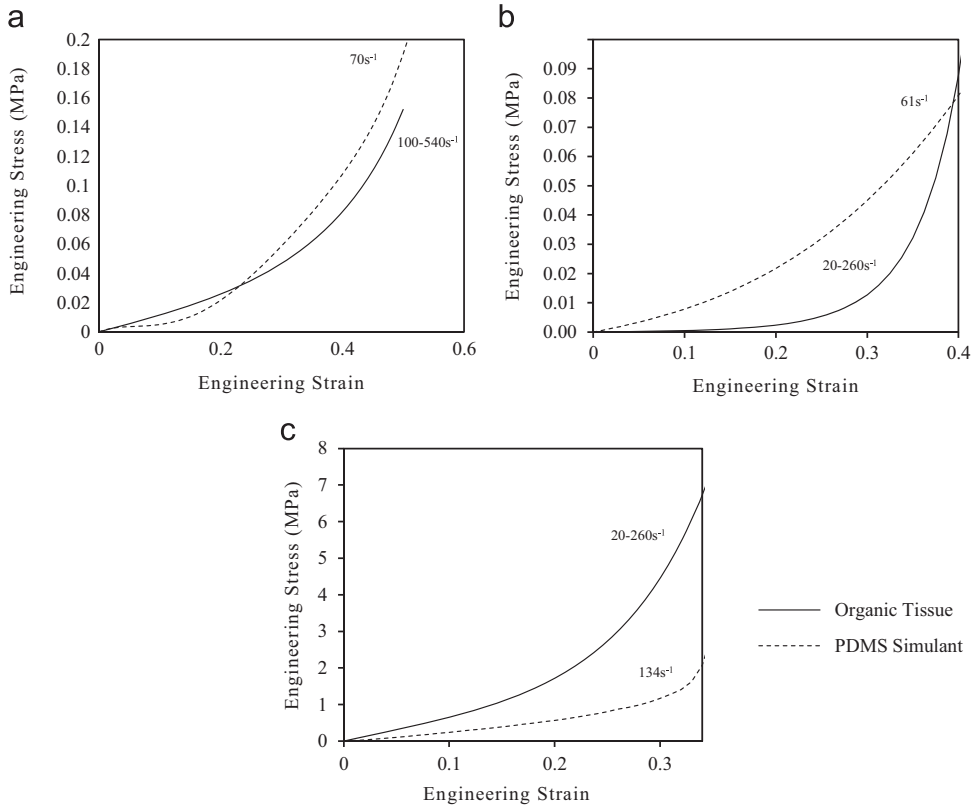

Fig. 11 – Engineering stress–strain graphs showing the organic tissue and PDMS simulant data used in FE simulations in (a) relaxed muscle; (b) subcutaneous tissue; and (c) skin.

Table 4 – Single term Ogden model coefficients for: skin (Shergold et al., 2006); adipose (Comley and Fleck, 2012); relaxed muscle (Mcelhaney, 1966; Song et al., 2007); cortical bone (Mcelhaney, 1966) and material densities for each organic tissue.

	μ	α	ρ
Skin	2.20×10^6	12	1110 (Mendez and Keys, 1960; Ward and Lieber, 2005)
Adipose	1.70×10^3	23	1100 (Sarvazyan et al., 1998)
Relaxed muscle	3.63×10^4	45	920 (Fidanza et al., 1953; Farvid et al., 2005)
Cortical bone	4.58×10^9	25	1880 (Yeni et al., 1998)

Table 5 – Prony series coefficients for organic skin, adipose and relaxed muscle tissues.

i	g(i)	k(i)	τ(i)
Skin			
1	5.01×10^1	3.80×10^{-1}	5.73×10^{-1}
2	4.44×10^{-1}	5.59×10^{-1}	9.47
Adipose			
1	1.59×10^{-2}	0.00	7.83×10^{-5}
2	-7.97×10^{-2}	0.00	1.17×10^{-3}
3	5.89×10^{-1}	0.00	1.61
4	1.25×10^{-1}	0.00	7.29×10^1
Relaxed muscle			
1	3.39×10^{-1}	0.00	2.37
2	2.56×10^{-1}	0.00	7.02×10^1

2.3.5. *Model definition*

The 3D surrogate geometries were discretised using first order C3D8R hexagonal brick elements due to their low computational cost and high rate of convergence. The reduced number of integration points per element also alleviates convergence for nearly incompressible materials (Podnos et al., 2006). Due to the dynamic nature of impacts, mesh densities were refined dependent on their master and slave assignments. Slave surfaces were assigned a finer mesh density to prevent coarse mesh discretisation, element distortion and penetration of surfaces. To avoid hourglassing and artificial results, four continuum solid elements were created through the thickness of the skin layer, this was used in combination with enhanced hourglass control to stabilise the contact and reduce artificial energies. All meshes were checked to ensure the maximum angle was no greater than 120°, minimum angle was no less than 20° and the element size was not less than 50% of the target size. The tissue layers were assigned nominal element sizes of: 3 mm, 2 mm, 4 mm and 3 mm for skin, adipose, muscle and bone respectively (Fig. 13).

The impactor was treated as a rigid body due to the large difference in stiffness between the impactor and surrogate and the anticipated small magnitude of displacements. This increases the computational efficiency as no element calculations are required for the impactor body. The rigid body was

Table 6 – Hyperelastic and viscoelastic model coefficients for PDMS skin, adipose and relaxed muscle tissues.

	Mooney–Rivlin coefficients			Prony series		
	D_{10}	C_{01}	C_{10}	i	g(i)	τ(i)
PDMS muscle	–	4.25×10^2	1.57×10^4	1	1.28×10^{-1}	3.52×10^{-1}
				2	5.29×10^{-2}	8.07
				3	3.39×10^{-2}	7.61×10^1
PDMS adipose	–	2.55×10^3	9.19×10^3	1	1.39×10^{-1}	7.51×10^{-5}
				2	1.70×10^{-1}	3.07
				3	7.41×10^{-2}	7.9×10^1
	Ogden coefficients					
		μ	α			
PDMS skin	–	5.92×10^5	2.61	1	2.67×10^{-2}	8.51×10^{-1}
				2	8.07×10^{-3}	4.04×10^1

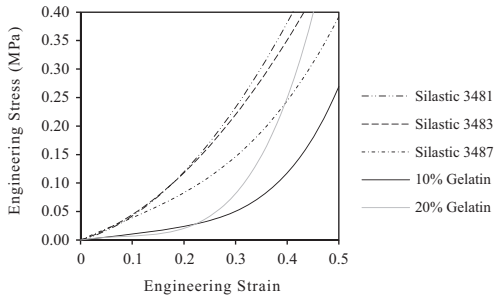

Fig. 12 – Compressive engineering stress–strain graphs of Silastic simulants and ballistics gelatin at representative intermediate strain rates (38-62s^{-1}).

discretised into 9834 tetrahedral elements, sufficient to maintain its geometric profile. Only the mass densities of the impactor were then required to govern their mechanical behaviour.

A surface-to-surface kinematic contact with pure master and slave surfaces was employed for the impactor and skin interaction. An exponential pressure-overclosure relationship was enforced defining normal behaviour with a pressure at zero overclosure of 100 kPa and a clearance at zero pressure of 1×10^{-4} m. A critical damping fraction of 0.1 was also employed in both the normal and tangential directions. A frictional coefficient of 0.75 was used to define the tangential behaviour with finite sliding parameters. The other tissue layers were tied together using the penalty method for reduced computational cost of the contact interaction and to represent the adhesion between tissue layers in the human body (e.g. skin and adipose). Previous organic tissue modelling studies have similarly considered the interactions between the bone–muscle and skin–fat layers in this manner (Rohan et al., 2013).

A time step of 0.04 s was used in the simulation with mass scaling to a minimum time increment of 1×10^{-6} s to reduce the computational time of interactions and prevent element distortion. The adipose layer experiences significantly greater strains than other tissues due to its softness. As a result, an element distortion control of 0.1 was employed in this layer, which will restrict the deformation of the elements at 0.9 nominal strain. It is noted that care must be taken when interpreting results with this artificial deformation constraint; however in this instance it is necessary for numerical stability and convergence. Wang et al. (2006) suggested that as a general rule the kinetic energy of the deforming material should not exceed a small fraction (5–10%) of the internal strain energy. The relative internal and artificial energies from the simulation is shown in Fig. 14.

3. Experimental validation of FE models

3.1. Background

To ensure that FE model predictions are accurate and believable, experimental validations have been performed. It is a common strategy to initially validate FE predictions against simplified structures and geometries and refine the findings to more complex systems (Tiossi et al., 2013).

3.2. Test methodology

Material drop tests were performed on a series of puck shaped surrogates simulating a high-mass, low-velocity knee-on-thigh human impact 130 mm diameter puck surrogates were fabricated for each of the simulant materials: Silastic 3481, 3483, 3487, 10% gelatin, 20% gelatin and PDMS formulations.

The impactor was dropped from a height of 0.5 m through a guidance system onto the puck surrogate, which was positioned on a Dytran 1061 V load cell (Dytran Instruments, USA). High speed imaging was also captured with a Photron Fastcam DA1 675K-C1 high-speed video camera (Photron Limited, USA) positioned perpendicular to the surrogate and recorded at 5000 frames per second with an image resolution of 1024×1024 pixels.

Four trials were conducted for each surrogate type with displacement–time and force–time outputs calculated from the video and load cell data. The experimental results were then compared with the predicted outputs from the FE models.

3.3. Validation results

Initial FE predictions indicated divergences of up to 42% from experimental data when using previously defined material

Table 7 – Hyperelastic Mooney–Rivlin and Ogden model coefficients and viscoelastic Prony series coefficients for single material simulants.

	Mooney–Rivlin coefficients			Prony series		
	D_{10}	C_{01}	C_{10}	i	g(i)	τ(i)
Silastic						
3481	–	6.11×10^4	1.35×10^4	1	6.17×10^{-2}	1.80×10^{-1}
				2	3.85×10^{-2}	5.55
				3	3.30×10^{-2}	9.61×10^{1}
3483	–	7.65×10^4	7.91×10^2	1	5.02×10^{-2}	2.18×10^{-1}
				2	2.87×10^{-2}	8.62
				3	2.60×10^{-2}	9.00×10^{1}
3487	–	5.31×10^4	1.59×10^3	1	5.52×10^{-2}	2.32×10^{-1}
				2	3.51×10^{-2}	8.80
				3	3.92×10^{-2}	8.81×10^{1}
	Ogden Coefficients					
	μ	*α*	*D*			
Ballistics gelatin						
10%	2.52×10^4	-2.93	2.26×10^5	1	2.27×10^{-1}	1.83
				2	3.88×10^{-1}	8.16×10^{1}
20%	17.3×10^4	-6.08	3.29×10^{-5}	1	1.56×10^{-1}	1.80
				2	3.89×10^{-1}	9.39×10^{1}

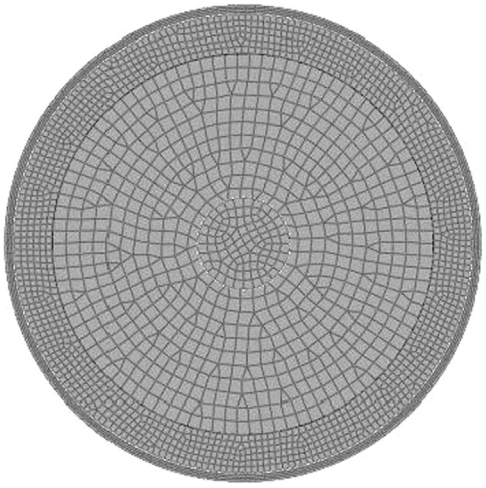

Fig. 13 – Cylindrical surrogate mesh density.

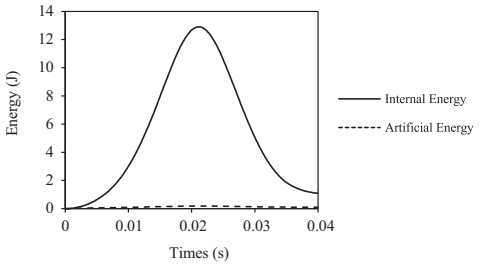

Fig. 14 – Artificial energy/internal energy vs. time graphs for knee impact in an organic tissue cylinder surrogate.

models. An investigation into the specific properties of the individual material batches used in the puck surrogates showed some process-induced variability (<15% stiffness) in mechanical response. The mechanical properties from the batch material were then used to populate the FE models. The FE model outputs attained have been compared to experimental data in Fig. 15 with the peak displacements (x_{max}), time to peak displacement (t_{max}), peak force (RF) and time to peak force (t_{rf}) presented in Table 8.

The 10% and 20% gelatin FE model predictions showed a significant divergence from the experimental test data both in terms of displacement and force parameters. Both models exhibited an increased stiffness, therefore the material models were optimised to provide a better representation of the experimental data. In both materials, the hyperelastic material stiffness was reduced to 1/3 of its original stiffness. The resultant model outputs are shown in Fig. 16 compared to experimental data.

4. Limb segment surrogate design analysis

4.1. *Introduction*

The responses of the developed PDMS simulants and single material soft tissue simulants were compared to predicted responses of an identical surrogate constructed from theoretically more biofidelic human tissues based upon the organic tissue material models detailed in Tables 4 and 5.

A series of mechanical response parameters were selected to evaluate the effectiveness of the limb segment surrogate. The maximum top surface displacement (x_{max}) and time to maximum deformation (t_x) were used as they provide a representation of the overall soft tissue response and the time over which it was achieved. This parameter provides an indication of the nett body segment deformation which relates to soft tissue injury modes and also affects the manner in which the body segment interacts with PPE. The maximal Cauchy stress, σ_{22}, normal to the direction of impact ($\sigma_{22,max}$) and time to peak stress (t_σ) were also recorded on the bone surface as they represent the magnitude of stresses transferred through the soft tissues. In an injury context, this parameter provides an indication of susceptibility to deep tissue injury and mechanical loading of the skeleton.

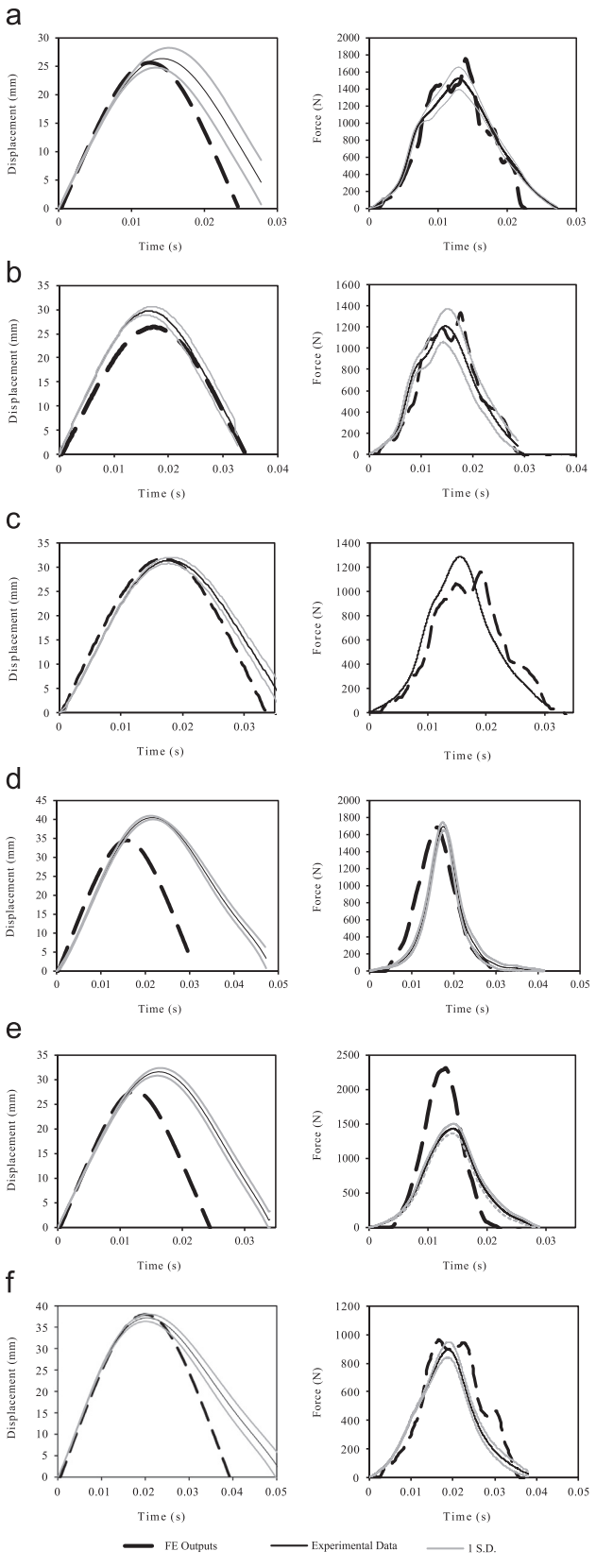

Fig. 15 – Displacement vs. time and force vs. time graphs showing a comparison between experimental results and FE model predictions for (a) Silastic 3481; (b) Silastic 3483; (c) Silastic 3487; (d) 10% Gelatin; (e) 20% Gelatin and (f) PDMS surrogates.

The maximum von Mises surface stresses ($\sigma_{v,max}$) and compressions for each of the layers are also a pertinent consideration as they are important to indicate the worth of a layered approach. The layer responses show the load transfer through the surrogate from the impact stimulus and the time course over which they occur. In a sports injury context, the layer effects also provide information on the susceptibility to surface or deep tissue damage and an indication of the differences in responses attained from different body types (e.g. athletic lean vs. sedentary fatty body types).

4.2. *Overall surrogate responses*

The maximum top surface displacements at each time interval and the peak stresses on the bone surface at each time interval are shown in Fig. 17a and b respectively.

The magnitudes of differences in x_{max}, t_x, $\sigma_{22,max}$ and t_σ are shown in Table 9 alongside percentage difference values from the idealised organic model predictions.

Sagittal plane sections of the surrogates taken at x_{max} for PDMS, organic tissues and the most representative single material simulant (10% gelatin) are displayed in Fig. 18 and show the magnitude of compression of the surrogates and associated tissue layers.

4.3. *Individual layer responses*

4.3.1. *Surface stresses*

The von Mises stresses ($\sigma_{v,max}$) experienced on the skin and muscle layer surfaces of the surrogates are shown in Fig. 19.

Fig. 19 shows $\sigma_{v,max}$ vs. time graphs for simulant materials on (a) skin layer surface and (b) muscle layer surface.

4.3.2. *Layer displacements*

The thicknesses of the tissue layers were compared between the organic tissue, PDMS, Silastic 3487 and 10% gelatin simulants throughout the knee impact in Fig. 20.

5. Discussion

5.1. *Organic tissue data*

Given the wide range of properties reported it is impossible to define absolutely the behaviour of human soft tissue. However, given representative data for a particular injury scenario (e.g. skin, adipose and muscle characterisation in an appropriate body segment, for a demographic of interest, over a relevant strain rate domain), this study explores whether superior synthetic materials can be developed to produce more biofidelic surrogates for experimental work and more biofidelic complementary constitutive models for computational analysis. The preceding study by Payne et al. (in press) collated organic muscle tissue data from Mcelhaney (1966) and Song et al. (2007) to provide a representative reference data set to act as a human muscle benchmark. The same approach has been adopted in the present study for skin and adipose tissues. Studies by Shergold et al. (2006) and Comley and Fleck (2012) provide an indication of the tissue behaviour under compressive loading conditions

Table 8 – Comparison of peak displacement (x_{max}), time to peak displacement (t_{max}) force (RF), time to peak force (t_{rf}) measurements between experimental data and FE model predictions.

	x_{max} (mm)		% Error	t_x (s)		% Error	RF (N)		% Error	t_{rf} (s)		% Error
	Exp.	FE		Exp.	FE		Exp.	FE		Exp.	FE	
PDMS Silicones	37.2	38.0	+2.04	0.0204	0.0200	−1.81	867	964	+7.72	0.0190	0.0166	−12.0
10% Gel	40.5	40.4	−0.20	0.0215	0.0178	−17.1	1694	1786	+5.38	0.0174	0.0178	+2.07
20% Gel	31.6	34.7	+9.78	0.0165	0.0154	−6.55	1435	1885	+31.3	0.0143	0.0158	+9.89
Silastic 3481	26.4	25.6	−2.77	0.0142	0.0126	−11.6	1526	1754	+14.9	0.0130	0.0129	−0.99
Silastic 3483	30.0	26.3	−11.2	0.0165	0.0172	+4.37	1210	1335	+10.3	0.0147	0.0176	+19.8
Silastic 3487	31.4	31.8	+1.27	0.0180	0.0170	−5.35	1288	1160	−9.89	0.0155	0.0192	+24.2

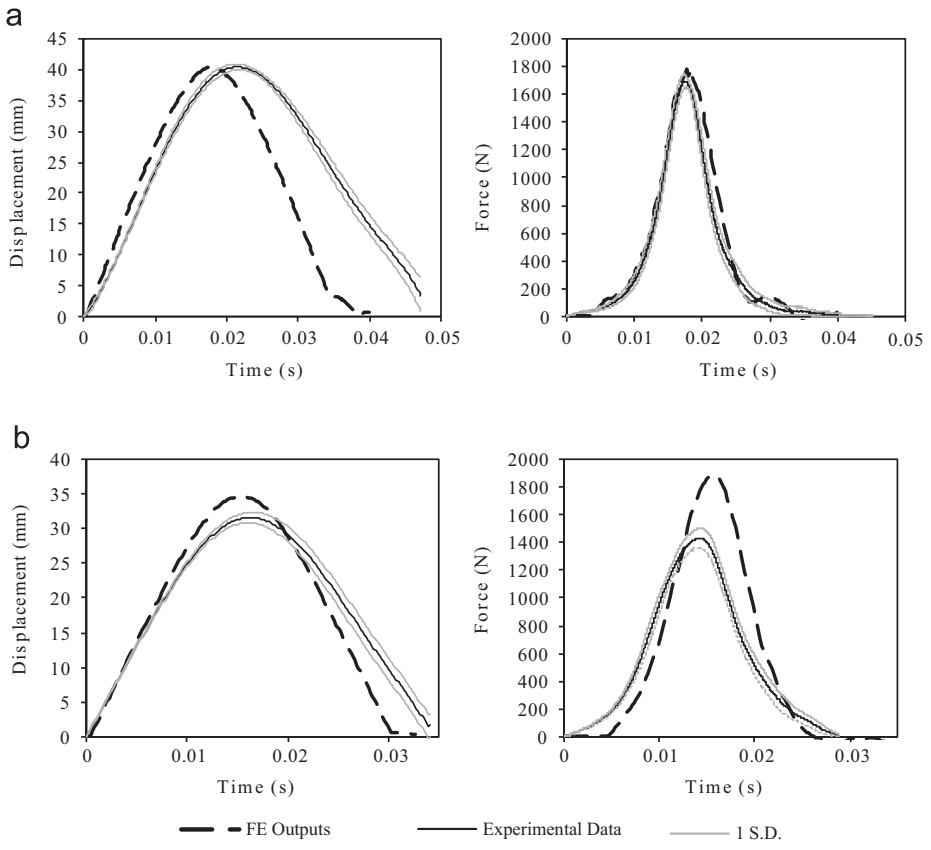

Fig. 16 – Displacement vs. time and force vs. time graphs showing a comparison between experimental results and optimised FE model predictions for (a) 10% Gelatin and (b) 20% Gelatin.

through a range of strain rates. Each of the tissues was considered as incompressible and isotropic as an initial simplification of their actual behaviour.

There is still, however, a lack data pertaining to the mechanical response of skin and adipose tissues under intermediate strain rates 50–1000 s^{-1}, particularly 250–1000 s^{-1} believed to be representative of the rates experienced from some sports impacts (e.g. cricket ball projectile). This introduces issues where the responses in this unreported region need to be inferred from data at unmatched strain rates. To better understand the responses of the organic tissues in the strain rate regions of interest further characterisation is required. Testing of organic tissues (e.g. porcine) under the same loading conditions used to characterise the PDMS silicones could provide more complete comparative data and a better confidence in the accuracy of the silicones. Nevertheless, the performance of the proposed PDMS formulations is promising.

5.2. *Adipose and skin tissue simulants*

5.2.1. *Quasi-static response*

The PDMS skin simulant exhibited a far lower stiffness than the organic tissue dataset at quasi-static strain rates but still provided an improved response compared to the best existing single soft tissue simulant tested (Silastic 3481). Errors of up to 89% were experienced between the PDMS simulant and organic tissues at 0.4 strain with a decreasing error to 86%

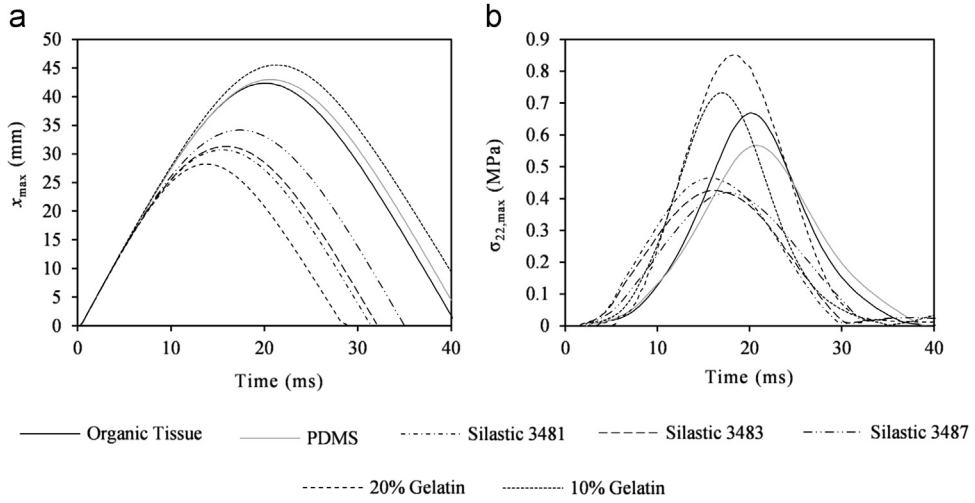

Fig. 17 – (a) x_{max} vs. time graph for top surrogate surface and (b) $\sigma_{22,max}$ vs. time graph on bone surface.

Table 9 – Maximum recorded displacement (x_{max}) and bone stress ($\sigma_{22,max}$) values for knee impact simulations (% difference from organic tissue predictions in brackets).

	Displacement		Bone stress	
	x_{max} (mm)	t_x (ms)	$\sigma_{22,max}$ (MPa)	t_σ (ms)
Organic tissues	42.3	20.0	0.669	20.0
PDMS silicones	42.9 (−1.42%)	20.6 (+3.00%)	0.567 (−15.2%)	20.8 (+4.00%)
10% Gel	45.5 (+7.57%)	21.2 (+6.00%)	0.733 (+9.57%)	17.0 (−15.0%)
20% Gel	28.2 (−33.3%)	13.8 (−31.0%)	0.852 (+27.4%)	18.6 (−7.00%)
Silastic 3481	30.7 (−27.4%)	15.5 (−22.5%)	0.465 (−30.5%)	15.5 (−22.5%)
Silastic 3483	31.3 (−26.0%)	16.0 (−20.0%)	0.426 (−36.3%)	16.0 (−20.0%)
Silastic 3487	34.1 (−13.5%)	17.3 (−13.5%)	0.419 (−37.4%)	17.5 (−12.5%)

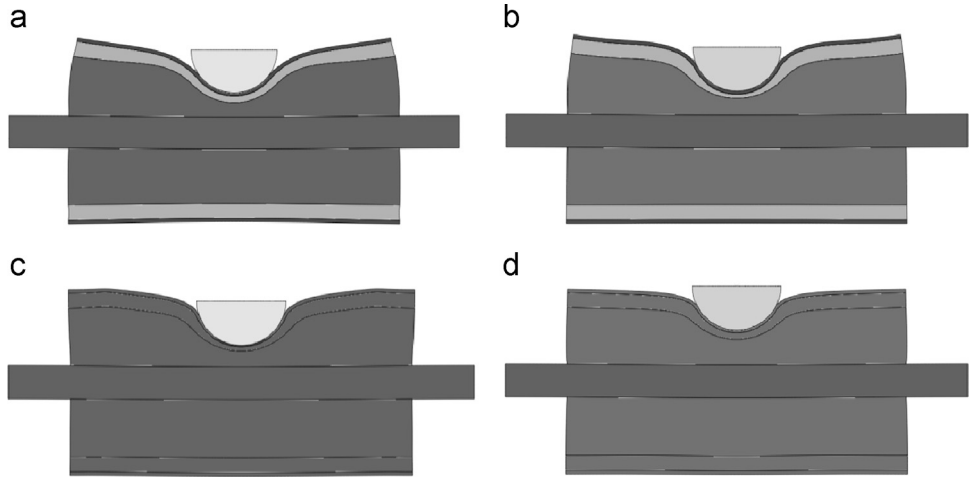

Fig. 18 – Images showing surrogate displacement in knee impact simulations in (a) organic tissues; (b) PDMS; (c) 10% gelatin; and (d) Silastic 3487.

at higher strains. The Silastic 3481 simulant exhibited an initial error of 89.2% increasing to 97% at 0.55 strain (Fig. 4). To achieve this modest improvement the PDMS formulation exhibited stiffness almost 3× greater than Silastic 3481 at 0.55 strain.

The developed PDMS silicones showed an improved quasi-static loading response to the most representative previously used simulants when compared to organic tissues. The PDMS adipose tissue simulant exhibited a 250% error initially at 0.1 strain and a decreasing error below 150% this point onwards. The best performing existing simulant (10% gelatin), showed a far greater divergence from the organic tissue dataset with an error of up to 1855% at 0.16 strain (Fig. 5). Generally, as noted in the previous study, the silicones tended to exhibit an

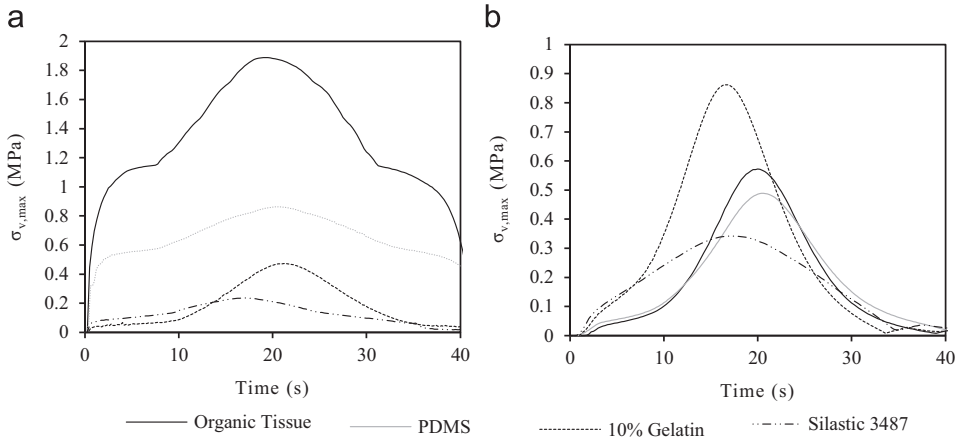

Fig. 19 – $\sigma_{v,max}$ vs. time graphs for simulant materials on (a) skin layer surface and (b) muscle layer surface.

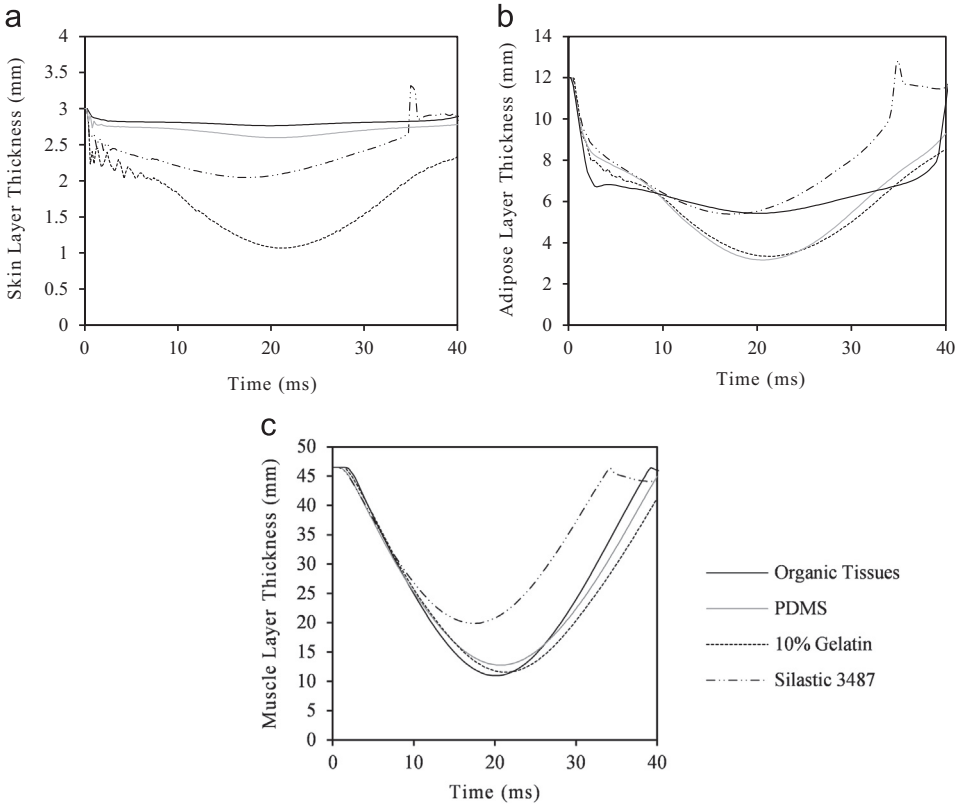

Fig. 20 – Tissue layer thicknesses showing responses through the knee impact simulation (a) skin; (b) adipose; and (c) muscle.

increased stiffness at low strains compared to organic tissues but exhibit a weaker strain hardening at higher strains.

5.2.2. *Intermediate strain rate response*

At increased strain rates the PDMS skin simulant showed a comparable magnitude of stiffness to organic tissues in similar strain rate ranges (Fig. 7). The PDMS adipose simulant, however, despite showing a more comparable quasi-static response experienced a significantly greater stiffness at increased strain rates within the reported range.

Both PDMS simulants exhibited significant strain rate dependencies, with their maximal stress response increasing by 12.5 × (0.4–194 s^{-1}) and 17 × (0.4–134 s^{-1}) in adipose and skin simulants at 0.5 and 0.3 strain respectively. Previous organic adipose characterisation studies have shown significant non-linear strain rate dependencies. Comley and Fleck (2012) reported a 4 × increase in maximal stress response between 0.2 s^{-1} and 250 s^{-1} and a 680 × increased stress response between 250 s^{-1} and 2700 s^{-1} at 0.3 strain. Similarly, Egelbrektsson (2011) reported an increase in maximal stress response of 2 × between 0.2 s^{-1} and 250 s^{-1}, and an increase of 1344 × between 250 s^{-1} and 2100 s^{-1} at 0.3 strain. The present study shows a considerably greater increase in maximal stress between quasi-static and approximately 250 s^{-1} strain rates. This is a factor that would need to be addressed in further iterations of the PDMS silicone

formulations and could potentially be developed for specific sports applications based on the relevant strain rate domains.

Organic skin characterisation studies have typically shown a lower strain rate dependency than adipose. Shergold et al. (2006) reported a 5× increase in maximal stress between 0.004 s^{-1} and 40 s^{-1}, and a 3.4× increase between 40 s^{-1} and 4000 s^{-1} at 0.4 strain in compression, whilst Lim et al. (2011) reported an increase in maximal stress of 3× between 0.004 s^{-1} and 1700 s^{-1} and an increase of at 1.5× between 1700 s^{-1} and 3700 s^{-1} at 0.2 strain in tension. By comparison, greater magnitudes of maximal stress increases were reported in developed PDMS skin than organic tissue. The initial differences between organic skin and the PDMS simulant under quasi-static loading conditions are compensated by a greater magnitude of strain hardening, which generates comparable behaviour. These results are in contrast to a those found by Shergold et al. (2006) who noted that porcine skin was more strain rate sensitive than silicone rubber and exhibited a greater stiffening at increased strain rates.

5.2.3. *Stress relaxation responses*

The viscoelastic properties of the PDMS silicones show large divergences from the organic tissues, in particular skin tissue is not well represented (Fig. 21). Organic skin exhibits significant viscoelastic behaviour, which could potentially be due to the movement of fibres and fluid, which are not present in the silicone structure. This perhaps indicates that the greatest future elastomer advances will not be achieved by revised elastomer formulations but by flexible composite material development instead.

5.3. *Computational model responses*

The combined multi-material surrogate responses from the developed PDMS silicones show a significantly improved representation of the predicted organic tissue responses than single material constructions using existing simulants.

The top surface displacements (Table 9) provide a good indication of the composite dynamic impact response behaviour of all of the tissue layers in combination. The PDMS silicones provided better matched levels of overall compression than single material constructions. A difference in x_{max} of −1.42% was recorded between the PDMS simulants and the target organic tissue model. The 10% gelatin simulant typically provided the closest representation of the x_{max} of the organic tissue model, however exhibited softer overall behaviour with a +7.57% difference from the organic tissue. The Silastic 3487 was the most comparable durable simulant, however exhibited an significantly increased stiffness and a difference in x_{max} of −27.4% from the organic tissue model predictions.

The σ_{22} stresses (Table 9) experienced on the bone are pertinent as they are a direct measure of the load transfer through the surrogate from the normal, axial impact. The PDMS silicones exhibited similar $\sigma_{22,max}$ profiles on the bone surface to the predicted organic tissue though showed −15.2% difference from the organic tissue model. The 10% gelatin model provided a closer representation of the $\sigma_{22,max}$ (+9.57%), though differed in t_σ by −15% compared to just +4% exhibited by the PDMS simulant model. The PDMS simulant model also more accurately represents the onset and delay in stresses predicted by the organic tissue model with a significantly elongated $\sigma_{22,max}$ −time trace to all other simulants.

The importance of a biofidelic skin layer was demonstrated in the surrogate model through $\sigma_{v,max}$ experienced on the top surface (Fig. 19a). The responses in the organic tissue and PDMS simulant models show comparable stress profiles with an initial sharp increase in stress followed by a gradual rise to the peak whilst all other simulants exhibited a more simple parabolic response. Although the PDMS skin exhibited a significantly reduced $\sigma_{v,max}$ compared to organic tissues it still provides a much closer match than other single material simulants. The importance of this layer is also emphasised by the lack of compression exhibited in the organic tissue and PDMS skin layers compared to other simulants (Fig. 20a).

The importance of a biofidelic adipose layer is highlighted by the initial rapid decreases in layer thickness shown in Fig. 20b. Organic adipose exhibits initially very soft behaviour with a rapidly increasing stiffness at approximately 0.3 strain (Section 1.2.2). The organic adipose tissue layer experiences greater initial levels of compression than the PDMS simulant. The PDMS simulant layer, however, experiences an overall greater level of compression than organic tissue, which could be attributed to the lower strain hardening present under high

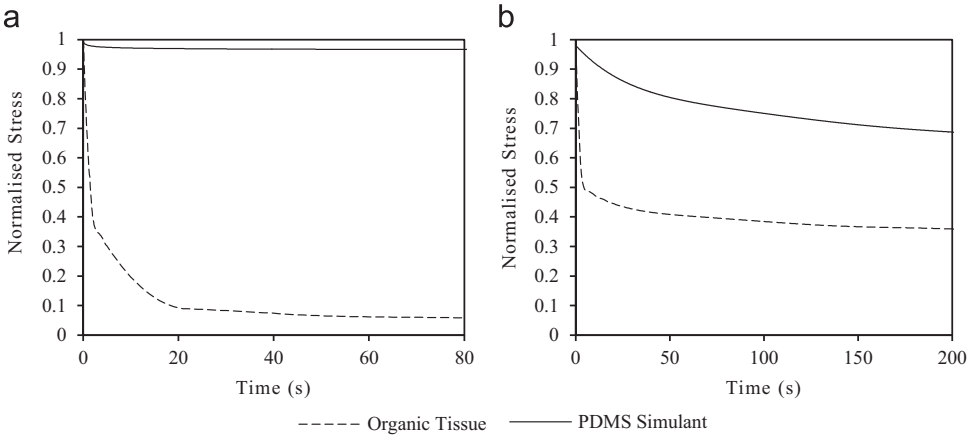

Fig. 21 – Normalised stress–time plots showing differences in stress relaxation between PDMS simulants and organic tissues in (a) skin (Wu et al., 2003); and (b) adipose (Gefen and Haberman, 2007) tissues.

strain deformations. The softer 10% gelatin simulant exhibits a slower initial displacement than the layered models but a similar level of overall compression to the PDMS simulant model.

Payne et al. (in press) indicated the relative benefits of a biofidelic muscle tissue simulant in uniaxial compression tests. Fig. 20c shows the thickness of the muscle tissue layers. The PDMS simulant model provided a close representation of the predicted organic tissue layer response exhibiting similar deformation responses and just a 16% difference at maximal compression. The $\sigma_{v,max}$ experienced on the muscle surface (Fig. 19b) also showed that the PDMS silicone exhibited the closest response to the predicted organic tissue model with −14.5% difference compared to a minimum of +50.7% difference in 10% gelatin surrogate.

Overall, the simulations showed that the PDMS silicone surrogate was the most biofidelic simulant for all geometries and loading conditions. The 10% gelatin simulant model was the best alternate single material simulant; however, this material is innately inappropriate for sports impact surrogates due to its frangibility. Frangible surrogates attain permanent damage from impacts, which are not suited to repeat testing required for PPE evaluations. Consequently, the surrogates are far more expensive per test than their mechanical alternatives and also often require specialised storage conditions and have limited shelf life. Silastic 3487 simulant provided the best existing durable synthetic representation of the multi-material response though still showed significant divergences from the target organic tissue predictions.

All the surrogate responses are compared to an idealised organic tissue model predicting how a human might behave under the same loading conditions. This is an essential aspect of the modelling approach and it is necessary to have a worthwhile and believable organic tissue model. Although, it is accepted that this is a simplification of actual human behaviour as some tissue complexities and interactions have been omitted. The best that can be achieved currently, to improve human surrogates, is to match our simplified understanding of organic tissue behaviour.

Previous studies which have examined human limb impact response have typically either examined the lower leg (Ankrah and Mills, 2003, 2004; Francisco et al., 2000), with particular regards to tibia impacts or considered high strain rate ballistic impacts (Bergeron et al., 2006). Hrysomallis (2009) reported a study of impact response of a human thigh segment (Hrysomallis, 2009), in which both human volunteers and cadavers were tested but further directly comparable data is scarce.

5.4. *External relevance of work*

An important application of such work is to relate the mechanical phenomena experienced by the surrogates to some measure of the likelihood of obtaining injuries. Information regarding the exact mechanical loading conditions or thresholds required to illicit particular injuries is vitally important. In sports, contusion injuries are often considered as the highest risk impact injury due to their frequency of occurrence (Crisco et al., 1994; Khattak et al., 2010; Smith et al., 2008), whilst fractures and lacerations are also pertinent considerations.

Contusions are widely considered to be caused by blunt non-penetrating trauma (Crisco et al., 1996) and resulting compression of soft tissues against the bone (Walton and Rothwell, 1983). Due to ethical constraints, however, little is known about in vivo organic tissue response to impact and the pathophysiological sequalae succeeding it. Previous studies have typically utilised mechanical drop test procedures on the hind limbs of anaesthetised rodents and have investigated regenerative aids to reduce the long term severity of resulting injuries. Few studies have investigated the mechanical causation for contusions (Crisco et al. 1994, 1996; Sherman et al. 2007; Mcbrier et al., 2009; Desmoulin and Anderson, 2011), with only a single study studying the onset in humans (Desmoulin and Anderson, 2011).

Existing studies lack comparable control over their inputs in terms of masses and drop heights used and are therefore difficult to compare or correlate meaningfully. In terms of physical measures to quantify the onset of contusions, whilst excessive strain is considered to be the injury mechanism, there is little consensus on which indirect mechanical phenomenon value (e.g. force, pressure) to consider (Beiner and Jokl, 2001). Ankrah and Mills (2004) suggested a value of 1 MPa could be considered as a metric to represent the onset of contusions, however a recent study by Desmoulin and Anderson (2011) showed a human participant experienced far greater pressures (up to 4.52 MPa) without a visible bruise. One of the main issues with such approaches are that there are no common measures for evaluating the effects of the impacts; Desmoulin and Anderson (2011), qualitatively assessed the size and colour of bruises, though this is suggested to be very site dependent and can vary based on the capillary densities. Other approaches have used MRI to identify specific tissue damage (Mcbrier et al., 2009), though the distinction between severities of contusions are similarly not well defined.

Studies to further identify the mechanical factors causing injury would be greatly influential and informative in this research but without surrogates or models that produce biofidelic stress or strain responses this is difficult. Arguably, the ability of manufacturers to accurately predict or assess the performance of PPE design with respect to injury phenomenon is also similarly restricted without better simulants, surrogates and models. Superior surrogates at least provide PPE designers with a more accurate means to empirically access the relative merits of different designs in anticipation of greater future certainty as to which mechanical response phenomena is most critical.

5.5. *Future developments*

Further iterations of the PDMS silicones must address methods to overcome the increased stiffness of the adipose simulant at higher strain rates and reduced stiffness of skin tissue under quasi-static loading conditions. The differences in rate dependencies between the silicones and organic tissues suggest that it may be beneficial to develop bespoke blends of silicone to match specific strain rate applications. In addition, the further complexity introduced

through consideration of organic tissue anisotropy is a factor which could potentially increase the biofidelity of the developed simulants. The ageing of skin is another pertinent consideration which affects the mechanical properties of the organic tissue (Pailler-Mattei et al., 2014). This could change human mechanical response to impact and injury tolerance levels and represent an area of potential further study.

Further study may also consider the Payne effect, which is a strain softening effect present in filled elastomers at low strain amplitudes in which an energy loss is observed due to filler–filler interactions. This could potentially affect the manner in which the materials behave under different impact conditions. Due to the high strains associated with sports blunt trauma impacts, this is not expected to be a significant issue; however this effect could be addressed more explicitly in future iterations of the PDMS silicones.

The characterisation of the PDMS simulants under a wider range of strain rates, particularly those pertinent to high rate projectile impacts are also an important area for future research and will enhance confidence in the FE models instead of extrapolating responses from lower rate experiments. This would enable more accurate dynamic FE analyses of the materials as projectile impacts can reach up to 34.6 ms^{-1} in relevant sports applications (Penrose et al., 1976). Given the high strain rate dependencies of the PDMS simulants and organic tissues, an investigation of surrogate impact behaviour under these higher strain rate conditions is important and could potentially require different PDMS blends for particular strain rate or sports applications.

Although the cylinder geometry used in this study embodied human anthropometric values they still represent large simplifications of actual human morphologies. There exist many levels of increasing geometric complexity and constraint that have not yet been considered. The differences in shape and tissue layer thicknesses in professional athletes are another factor that requires consideration, as well as more biofidelic human constraints.

To generate the computational model several assumptions were required, ranging from the isotropic stress–strain behaviour of the tissues under varying strain rates imposed to the level of adhesion between tissue structures. The puck surrogates were validated against experimental data, to establish confidence in the cylindrical thigh model response predictions. A similar validation and optimisation study could be conducted to further validate this model.

The parallel development of synthetic and computational human surrogates will provide further validation and confidence in each approach. The continued development of these technologies provides scope for more biofidelic improved surrogate models.

6. Conclusions

This study presents a multi-material human tissue surrogate development approach using additive cure PDMS soft tissues. Target organic tissue properties were established from previous uniaxial compressive tests on skin and adipose tissues and used as a guideline to develop synthetic additive cure PDMS simulants, which were tested through a range of strain rates. Constitutive models were established describing the hyperelastic and viscoelastic behaviour of the simulants which were used in FE models and validated using experimental data from associated drop tests. The FE responses were compared to organic tissue properties and previously used simulants. The new PDMS simulants provided a superior approximation of the predicted organic tissue response than previously used single material soft tissue synthetic simulants.

REFERENCES

Albright, A.L., Stern, J.S., 1998. Adipose Tissue, Encyclopedia of Sports Medicine and Science. In: Fahey, T.D. (Ed.), Internet Society for Sport Science (http://sportsci.org)).

Alkhouli, N., Mansfield, J., Green, E., Bell, J., Knight, B., Liversedge, N., Tham, J.C., Welbourn, R., Shore, A.C., Kos, K., Winlove, C.P., 2013. The mechanical properties of human adipose tissues and their relationships to the structure and composition of the extracellular matrix. Am. J. Physiol. Endocrinol. Metab. 305 (12), E1427–E1435 (DOI:10.1152/ajpendo.00111.2013; 10.1152/ajpendo.00111.2013).

Ankersen, J., Birkbeck, A., Thomson, R., Vanezis, P., 1999. Puncture resistance and tensile strength of skin simulants. Proc. Inst. Mech. Eng. Part H: J. Eng. Med. 213 (6), 493–501, http://dx.doi.org/10.1243/0954411991535103.

Ankrah, S., Mills, N., 2003. Performance of football shin guards for direct stud impacts. Sports Eng. 6 (4), 207–219, http://dx.doi.org/10.1007/BF02844024.

Ankrah, S., Mills, N., 2004. Analysis of ankle protection in Association football. Sports Eng. 7 (1), 41–52, http://dx.doi.org/10.1007/BF02843972.

Avon, S., Wood, R., 2005. Porcine skin as an in vivo model for ageing of human bite marks. J. Forensic Odontostomatol. 23 (2), 30–39.

Azar, F.S., Metaxas, D.N., Schnall, M.D., 2002. Methods for modeling and predicting mechanical deformations of the breast under external perturbations. Med. Image Anal. 6 (1), 1–27, http://dx.doi.org/10.1016/S1361-8415(01)00053-6.

Beiner, J.M., Jokl, P., 2001. Muscle contusion injuries: current treatment options. J. Am. Acad. Orthop. Surg. 9 (4), 227–237.

Bergeron, D.M., Anderson, I.B., Coley, C.G., Fall, R.W., 2006. Assessment of Lower Leg Injury from Land Mine Blast – Phase 1: Test Results using a Frangible Surrogate Leg with Assorted Protective Footwear and Comparison with Cadaver Test Data. DRDC Suffield TR 2006-051. Defence Research and Development Canada, Valcartier, Canada.

Brown, I.A., 1973. A scanning electron microscope study of the effects of uniaxial tension on human skin. Br. J. Dermatol. 89 (4), 383–393, http://dx.doi.org/10.1111/j.1365-2133.1973.tb02993.x.

Cohen, R., Hooley, C., Mccrum, N., 1976. Viscoelastic creep of collagenous tissue. J. Biomech. 9 (4), 175–184, http://dx.doi.org/10.1016/0021-9290(76)90002-6.

Comley, K., Fleck, N., 2012. The compressive response of porcine adipose tissue from low to high strain rate. Int. J. Impact Eng. 46, 1–10, http://dx.doi.org/10.1016/j.ijimpeng.2011.12.009.

Comley, K., Fleck, N.A., 2010. A micromechanical model for the Young's modulus of adipose tissue. Int. J. Solids Struct. 47 (21), 2982–2990, http://dx.doi.org/10.1016/j.ijsolstr.2010.07.001.

Crisco, J., Hentel, K., Jackson, W., Goehner, K., Jokl, P., 1996. Maximal contraction lessens impact response in a muscle contusion model. J. Biomech. 29 (10), 1291–1296, http://dx.doi.org/10.1016/0021-9290(96)00047-4.

Crisco, J.J., Jokl, P., Heinen, G.T., Connell, M.D., Panjabi, M.M., 1994. A muscle contusion injury model. Biomechanics, physiology, and histology. Am. J. Sports Med. 22 (5), 702–710, http://dx.doi.org/10.1177/036354659402200521.

Desmoulin, G.T., Anderson, G.S., 2011. Method to investigate contusion mechanics in living humans. J. Forensic Biomech. 2 (1), 1–10.

Douglas, W.R., 1972. Of pigs and men and research: a review of applications and analogies of the pig, sus scrofa, in human medical research. Sp. Life. Sci. 3 (3), 226–234, http://dx.doi.org/10.1007/BF00928167.

Dunn, M.G., Silver, F.H., Swann, D.A., 1985. Mechanical analysis of hypertrophic scar tissue: structural basis for apparent increased rigidity. J. Invest. Dermatol. 84 (1), 9–13, http://dx.doi.org/10.1111/1523-1747.ep12274528.

Edwards, C., Marks, R., 1995. Evaluation of biomechanical properties of human skin. Clin. Dermatol. 13 (4), 375–380, http://dx.doi.org/10.1016/0738-081X(95)00078-T.

Egelbrektsson, K., 2011. *Evaluation of material models in LS-DYNA for impact simulation of white adipose tissue*, Masters Thesis, Chalmers University of Technology.

Erdemir, A., Viveiros, M.L., Ulbrecht, J.S., Cavanagh, P.R., 2006. An inverse finite-element model of heel-pad indentation. J. Biomech. 39 (7), 1279–1286, http://dx.doi.org/10.1016/j.jbiomech.2005.03.007.

Fackler, M.L., 1988. Ordnance gelatin for ballistic studies: Detrimental effect of excess heat used in gelatin preparation. Am. J. Forensic Med. Pathol. 9 (3), 218–219, http://dx.doi.org/10.1097/00000433-198809000-00008.

Farvid, M., Ng, T., Chan, D., Barrett, P., Watts, G., 2005. Association of adiponectin and resistin with adipose tissue compartments, insulin resistance and dyslipidaemia. Diab. Obes. Metab. 7 (4), 406–413, http://dx.doi.org/10.1111/j.1463–1326.2004.00410.x.

Fidanza, F., Keys, A., Anderson, J.T., 1953. Density of body fat in man and other mammals. J. Appl. Physiol. 6 (4), 252–256.

Finlay, J.B., 1978. Thixotropy in human skin. J. Biomech. 11 (6), 333–342, http://dx.doi.org/10.1016/0021-9290(78)90066-0.

Flynn, C., Mccormack, B.A., 2008. Finite element modelling of forearm skin wrinkling. Skin Res. Technol. 14 (3), 261–269, http://dx.doi.org/10.1111/j.1600-0846.2008.00289.x.

Fontanella, C., Matteoli, S., Carniel, E., Wilhjelm, J.E., Virga, A., Corvi, A., Natali, A., 2012. Investigation on the load-displacement curves of a human healthy heel pad: in vivo compression data compared to numerical results. Med. Eng. Phys. 34 (9), 1253–1259, http://dx.doi.org/10.1016/j.medengphy.2011.12.013.

Francisco, A.C., Nightingale, R.W., Guilak, F., Glisson, R.R., Garrett Jr, W.E., 2000. Comparison of soccer shin guards in preventing tibia fracture. Am. J. Sports Med. 28 (2), 227–233.

Gallagher, A., Ní Annaidh, A., Bruyère, K., 2012. Dynamic tensile properties of human skin. In: Proceedings of the 2012 International Research Council on the Biomechanics of Injury, 12–14 September 2012, pp. 494–502.

Geerligs, M., Peters, G.W., Ackermans, P.A., Oomens, C.W., Baaijens, F.P., 2008. Linear viscoelastic behavior of subcutaneous adipose tissue. Biorheology 45 (6), 677–688, http://dx.doi.org/10.3233/BIR-2008-0517.

Gefen, A., Haberman, E., 2007. Viscoelastic properties of ovine adipose tissue covering the gluteus muscles. J. Biomech. Eng. 129 (6), 924–930, http://dx.doi.org/10.1115/1.2800830.

Goldsmith, L.A., 1990. My organ is bigger than your organ. Arch. Dermatol. 126 (3), 301–302, http://dx.doi.org/10.1001/archderm.1990.01670270033005.

Halkon, B.J., Mitchell, S.R., Payne, T., Carbo, J., 2014. The biomechanics of human impacts in basketball. Proc. Eng. 72, 214–219, http://dx.doi.org/10.1016/j.proeng.2014.06.038.

Haut, R., 1989. The effects of orientation and location on the strength of dorsal rat skin in high and low speed tensile failure experiments. J. Biomech. Eng. 111 (2), 136–140, http://dx.doi.org/10.1115/1.3168354.

Holzapfel, G.A., 2004. Computational biomechanics of soft biological tissue, Encylclopedia of Computational Mechanics. Wiley Online Library, Graz, Austria.

Hrysomallis, C., 2009. Surrogate thigh model for assessing impact force attenuation of protective pads. J. Sci. Med. Sport 12 (1), 35–41, http://dx.doi.org/10.1016/j.jsams.2007.07.013.

Jamison, C., Marangoni, R., Glaser, A., 1968. Viscoelastic properties of soft tissue by discrete model characterization. J. Biomech. 1 (1), 33–46, http://dx.doi.org/10.1016/0021-9290(68)90036-5.

Jee, T., Komvopoulos, K., 2014. Skin viscoelasticity studied in vitro by microprobe-based techniques. J. Biomech. 47 (2), 553–559, http://dx.doi.org/10.1016/j.jbiomech.2013.10.006.

Jussila, J., 2004. Preparing ballistic gelatine – review and proposal for a standard method. Forensic Sci. Int. 141 (2), 91–98, http://dx.doi.org/10.1016/j.forsciint.2003.11.036.

Khattak, M.J., Ahmad, T., Rehman, R., Umer, M., Hasan, S.H., Ahmed, M., 2010. Muscle healing and nerve regeneration in a muscle contusion model in the rat. J. Bone Joint Surg. Br. Vol. 92 (6), 894–899, http://dx.doi.org/10.1302/0301-620X.92B6.22819.

Krouskop, T.A., Wheeler, T.M., Kallel, F., Garra, B.S., Hall, T., 1998. Elastic moduli of breast and prostate tissues under compression. Ultrason. Imaging 20 (4), 260–274, http://dx.doi.org/10.1177/016173469802000403.

Lanir, Y., Fung, Y., 1974. Two-dimensional mechanical properties of rabbit skin – I. Experimental system. J. Biomech. 7 (1), 29–34, http://dx.doi.org/10.1016/0021-9290(74)90067-0.

Lim, J., Hong, J., Chen, W.W., Weerasooriya, T., 2011. Mechanical response of pig skin under dynamic tensile loading. Int. J. Impact Eng. 38 (2), 130–135, http://dx.doi.org/10.1016/j.ijimpeng.2010.09.003.

Liu, Z., Yeung, K., 2008. The preconditioning and stress relaxation of skin tissue. J. Biomed. Pharmaceut. Eng. 2 (1), 22–28.

Mcbrier, N.M., Neuberger, T., Okita, N., Webb, A., Sharkey, N., 2009. Reliability and validity of a novel muscle contusion device. J. Athl. Train. 44 (3), 275–278, http://dx.doi.org/10.4085/1062-6050-44.3.275.

Mcelhaney, J.H., 1966. Dynamic response of bone and muscle tissue. J. Appl. Physiol. 21 (4), 1231–1236.

Mendez, J., Keys, A., 1960. Density and composition of mammalian muscle. Metabolism 9 (2), 184–188.

Miller-Young, J.E., Duncan, N.A., Baroud, G., 2002. Material properties of the human calcaneal fat pad in compression: experiment and theory. J. Biomech. 35 (12), 1523–1531, http://dx.doi.org/10.1016/S0021-9290(02)00090-8.

Natali, A., Fontanella, C., Carniel, E., 2012. A numerical model for investigating the mechanics of calcaneal fat pad region. J. Mech. Behav. Biomed. Mater. 5 (1), 216–223, http://dx.doi.org/10.1016/j.jmbbm.2011.08.025.

Ní Annaidh, A., Bruyère, K., Destrade, M., Gilchrist, M.D., Otténio, M., 2012. Characterization of the anisotropic mechanical properties of excised human skin. J. Mech. Behav. Biomed. Mater. 5 (1), 139–148, http://dx.doi.org/10.1016/j.jmbbm.2011.08.016.

Pailler-Mattei, C., Bec, S., Zahouani, H., 2008. In vivo measurements of the elastic mechanical properties of human skin by indentation tests. Med. Eng. Phys. 30 (5), 599–606, http://dx.doi.org/10.1016/j.medengphy.2007.06.011.

Pailler-Mattei, C., Laquièze, L., Debret, R., Tupin, S., Aimond, G., Sommer, P., Zahouani, H., 2014. Rheological behaviour of reconstructed skin. J. Mech. Behav. Biomed. Mater. 37, 251–263, http://dx.doi.org/10.1016/j.jmbbm.2014.05.030.

Paus, R., Klein, J., Permana, P., Owecki, M., Chaldakov, G., Böhm, M., Hausman, G., Lapière, C., Atanassova, P., Sowiński, J., 2007.

What are subcutaneous adipocytes really good for…?. Exp. Dermatol. 16 (1), 45–47, http://dx.doi.org/10.1111/j.1600-0625.2006.00519_1.x.

Payne T., Mitchell S.R., Bibb R. and Waters M., Development of novel synthetic muscle tissues for sports impact surrogates, J. Mech. Behav. Biomed. Mater. http://dx.doi.org/10.1016/j.jmbbm.2014.08.011, in press.

Payne, T., Mitchell, S., Bibb, R., 2013. Design of human surrogates for the study of biomechanical injury: a review. Crit. Rev.™ Biomed. Eng. 41 (1), 51-89, http://dx.doi.org/10.1615/CritRevBiomedEng.2013006847.

Penrose, T., Foster, D., Blanksby, B., 1976. Release velocities of fast bowlers during a cricket test match. Aust. J. Health Phys. Educ. Recreat. 71 (Suppl.), S2–S5.

Podnos, E., Becker, E., Klawitter, J., Strzepa, P., 2006. FEA analysis of silicone MCP implant. J. Biomech. 39 (7), 1217–1226, http://dx.doi.org/10.1016/j.jbiomech.2005.03.019.

Potts, R.O., Buras Jr, E.M., Chrisman Jr, D.A., 1984. Changes with age in the moisture content of human skin. J. Invest. Dermatol. 82 (1), 97–100, http://dx.doi.org/10.1111/1523-1747.ep12259203.

Rho, J.Y., Ashman, R.B., Turner, C.H., 1993. Young's modulus of trabecular and cortical bone material: ultrasonic and microtensile measurements. J. Biomech. 26 (2), 111–119, http://dx.doi.org/10.1016/0021-9290(93)90042-D.

Robbins, S.E., Gouw, G.J., Hanna, A.M., 1989. Running-related injury prevention through innate impact-moderating behavior. Med. Sci. Sports Exerc. 21 (2), 130–139.

Rohan, C., Badel, P., Lun, B., Rastel, D., Avril, S., 2013. Biomechanical response of varicose veins to elastic compression: a numerical study. J. Biomech. 46 (3), 599–603, http://dx.doi.org/10.1016/j.jbiomech.2012.10.043.

Samani, A., Plewes, D., 2004. A method to measure the hyperelastic parameters of ex vivo breast tissue samples. Phys. Med. Biol. 49 (18), 4395–4405, http://dx.doi.org/10.1088/0031-9155/49/18/014.

Samani, A., Zubovits, J., Plewes, D., 2007. Elastic moduli of normal and pathological human breast tissues: an inversion-technique-based investigation of 169 samples. Phys. Med. Biol. 52 (6), 1565–1576, http://dx.doi.org/10.1088/0031-9155/52/6/002.

Samani, A., Bishop, J., Luginbuhl, C., Plewes, D.B., 2003. Measuring the elastic modulus of ex vivo small tissue samples. Phys. Med. Biol. 48 (14), 2183–2198, http://dx.doi.org/10.1088/0031-9155/48/14/310.

Sapozhnikov, S., Ignatova, A., 2013. Experimental and theoretical investigation of deformation and fracture of subcutaneous fat under compression. Mech. Compos. Mater. 48 (6), 649–654, http://dx.doi.org/10.1007/s11029-013-9309-7.

Sarvazyan, A.P., Goukassian, D., Maevsky, E., Oranskara, G., 1994. Elasticity imaging as a new modality of medical imaging for cancer detection. In: Proceedings of the International Workshop "Interaction of Ultrasound with Biological Media" 1994, Valenciennes, France, pp. 69–81.

Sarvazyan, A.P., Rudenko, O.V., Swanson, S.D., Fowlkes, J.B., Emelianov, S.Y., 1998. Shear wave elasticity imaging: a new ultrasonic technology of medical diagnostics. Ultrasound Med. Biol. 24 (9), 1419–1435 (DOI:0.1016/S0301-5629(98)00110-0).

Schmook, F.P., Meingassner, J.G., Billich, A., 2001. Comparison of human skin or epidermis models with human and animal skin in in-vitro percutaneous absorption. Int. J. Pharm. 215 (1), 51–56, http://dx.doi.org/10.1016/S0378-5173(00)00665-7.

Sellier, K.G., Kneubuehl, B.P., 1994. Wound Ballistics and the Scientific Background. Elsevier Science Health Science Div., New York.

Shergold, O.A., Fleck, N.A., Radford, D., 2006. The uniaxial stress versus strain response of pig skin and silicone rubber at low and high strain rates. Int. J. Impact Eng. 32 (9), 1384–1402, http://dx.doi.org/10.1016/j.ijimpeng.2004.11.010.

Sherman, D., Bir, C., Viano, D., Haacke, E.M., 2007. Evaluation and Quantification of Bruising. International Society of Biomechanics XXth Congress – ASB 29th Annual Meeting, Cleeveland, Ohio, July 31–August 5, 2007, p. 700.

Sims, A., Stait-Gardner, T., Fong, L., Morley, J., Price, W., Hoffman, M., Simmons, A., Schindhelm, K., 2010. Elastic and viscoelastic properties of porcine subdermal fat using MRI and inverse FEA. Biomech. Model. Mechanobiol. 9 (6), 703–711, http://dx.doi.org/10.1007/s10237-010-0207-9.

Smith, C., Kruger, M.J., Smith, R.M., Myburgh, K.H., 2008. The inflammatory response to skeletal muscle injury. Sports Med. 38 (11), 947–969, http://dx.doi.org/10.2165/00007256-200838110-00005.

Sommer, G., Eder, M., Kovacs, L., Pathak, H., Bonitz, L., Mueller, C., Regitnig, P., Holzapfel, G.A., 2013. Multiaxial mechanical properties and constitutive modeling of human adipose tissue: a basis for preoperative simulations in plastic and reconstructive surgery. Acta Biomater. 9 (11), 9036–9048, http://dx.doi.org/10.1016/j.actbio.2013.06.011.

Song, B., Chen, W., Ge, Y., Weerasooriya, T., 2007. Dynamic and quasi-static compressive response of porcine muscle. J. Biomech. 40 (13), 2999–3005, http://dx.doi.org/10.1016/j.jbiomech.2007.02.001.

Sugihara, T., Ohura, T., Homma, K., Igawa, H., 1991. The extensibility in human skin: variation according to age and site. Br. J. Plast. Surg. 44 (6), 418–422, http://dx.doi.org/10.1016/0007-1226(91)90199-T.

Tiossi, R., Vasco, M.A., Lin, L., Conrad, H.J., Bezzon, O.L., Ribeiro, R. F., Fok, A.S., 2013. Validation of finite element models for strain analysis of implant-supported prostheses using digital image correlation. Dent. Mater. 29 (7), 788–796, http://dx.doi.org/10.1016/j.dental.2013.04.010.

Van Houten, E.E.W., Doyley, M.M., Kennedy, F.E., Weaver, J.B., Paulsen, K.D., 2003. Initial in vivo experience with steady-state subzone-based MR elastography of the human breast. J. Magn. Reson. Imaging 17 (1), 72–85, http://dx.doi.org/10.1002/jmri.10232.

Van Loocke, M., Simms, C., Lyons, C., 2009. Viscoelastic properties of passive skeletal muscle in compression—Cyclic behaviour. J. Biomech. 42 (8), 1038–1048, http://dx.doi.org/10.1016/j.jbiomech.2009.02.022.

Walton, M., Rothwell, A.G., 1983. Reactions of thigh tissues of sheep to blunt trauma. Clin. Orthop. Relat. Res. 176, 273–281, http://dx.doi.org/10.1097/00003086-198306000-00040.

Wang, M., Yang, H., Sun, Z., Guo, L., Ou, X., 2006. Dynamic explicit FE modeling of hot ring rolling process. Trans. Nonferr. Metals Soc. China 16 (6), 1274–1280, http://dx.doi.org/10.1016/S1003-6326(07)60006-5.

Ward, S.R., Lieber, R.L., 2005. Density and hydration of fresh and fixed human skeletal muscle. J. Biomech. 38 (11), 2317–2320, http://dx.doi.org/10.1016/j.jbiomech.2004.10.001.

Wu, J.Z., Dong, R.G., Smutz, W.P., Schopper, A.W., 2003. Nonlinear and viscoelastic characteristics of skin under compression: experiment and analysis. Biomed. Mater. Eng. 13 (4), 373–385.

Yeni, Y., Brown, C., Norman, T., 1998. Influence of bone composition and apparent density on fracture toughness of the human femur and tibia. Bone 22 (1), 79–84, http://dx.doi.org/10.1016/S8756-3282(97)00227-5.

Young, D.A., Christman, K.L., 2012. Injectable biomaterials for adipose tissue engineering. Biomed. Mater. 7 (2), 024104, http://dx.doi.org/10.1088/1748-6041.